Table 2 Transmural dispersion of activity-recovery intervals before and after administration of epinephrine in the absence and presence of propranolol in the left and right ventricular walls

	Activation-recovery intervals		
	Before propranolol	After propranolol	*P* (Endo vs. Mid vs. Epi)
Left ventricle			
Before epinephrine	61 (4)	37 (2)	<0.001
After epinephrine	34 (3)	35 (2)	0.810
P (baseline vs. epinephrine)	<0.001	0.205	
Right ventricle			
Before epinephrine	18 (2)	17 (1)	0.851
After epinephrine	14 (2)	17 (2)	0.118
P (baseline vs. epinephrine)	0.148	0.905	

Values are means (SEM).

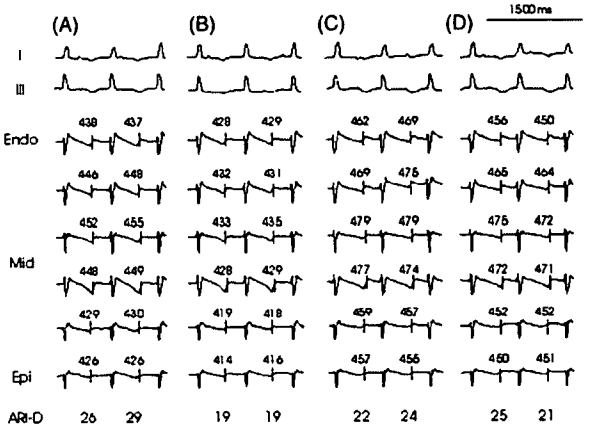

Figure 4 RV transmural electrograms. The display is as in *Figure 2*. At baseline (*A*), ARI at the Mid site is slightly longer than at the Epi and Endo sites, and ARI dispersion (ARI-D) is 26–29 ms. ARI was mildly shortened by epinephrine, 0.5 μg/kg (*B*). Propranolol prolonged ARI homogeneously (*C*) and ARI dispersion was 22–24 ms. The effects of epinephrine on the ARI distribution was reversed by propranolol (*D*). Abbreviations as in *Figure 1*.

The response of ventricular repolarization to adrenergic stimulation in the normal heart largely depends on the shift in net outward current. An increase in the net outward repolarization current, due to a relatively large increase in I_{Ks} and Ca^{2+}-activated chloride currents compared to the I_{Ca} and Na^+/Ca^{2+} exchange currents, is thought to be responsible for the shortening of ventricular repolarization by adrenergic stimulation.[20–22]

Conversely, in LQT1 and LQT2, adrenergic stimulation has been reported to induce continuous or transient prolongations of the QT interval, and an increased dispersion of ventricular repolarization.[6–8,23] These observations are closely related to the occurrence, in patients suffering from LQT1 and LQT2, of adverse cardiac events mostly associated with exercise, emotional stress, or both.[1,4,5] In contrast to its effects in LQT1 and LQT2, adrenergic stimulation is considered less arrhythmogenic in LQT3, as most adverse cardiac events occur at rest or during sleep.[1,4,5] Furthermore, in some experimental and clinical studies, adrenergic stimulation shortened the QT interval and lessened the dispersion of ventricular repolarization in LQT3.[6,7,23] These beneficial effects of adrenergic stimulation in LQT3, where an enhanced inward I_{Na} current is responsible for the prolongation of the QT interval, were attributed to an increase of the net outward current, mainly across normal I_{Ks} channels.[24,25] The results of this study, in a model of LQT3 created by AP-A, where ventricular ARI and transmural ARI dispersion were shortened by the administration of 0.5 μg/kg of epinephrine, are consistent with these previous observations.[6,7,23] However, when administered a higher dose, epinephrine was pro-arrhythmic in the majority of the experiments. Since (i) 1.0 μg/kg is a relevant dose clinically, (ii) it did not cause inordinately severe hypertension, and (iii) similar PVC, but not polymorphic VA were induced by the same dose of epinephrine before the administration of AP-A, adrenergic activity exhibits opposite effects on ventricular electrical stability in the LQT3 model, depending on the intensity of stimulation. Furthermore, this observation is consistent with the incidence, in LQT3, of certain adverse cardiac events occurring in association with exercise or emotional stress.[1,4,5]

Beta-adrenergic blockade in LQT3

Since VA in LQT3 are often bradycardia-dependent, beta-adrenergic blockade might be less effective or even harmful in this syndrome, as a slow heart rate can promote a more heterogeneous distribution of ventricular repolarization and facilitate the induction of triggered beats due to early after-depolarization.[26–28] However, supplemental treatment with a beta-adrenergic blocker has the potential to limit the incidence of VA episodes if bradycardia is prevented by a pacemaker or an implantable cardioverter defibrillator.[10] Previous studies using pharmacological models of an arterially perfused LV wedge, sliced myocardium, or ventricular cells have shown that beta-adrenergic blockade had little or no effect on the QT interval in several types of LQTS.[6–8] However, in this study, propranolol prolonged ARI at all sites, although the ARI prolongation was mild. The difference between the previous studies and ours might be partially explained by the effect of basal autonomic nerve activity. In this study, basal adrenergic activity appears to have augmented the net outward current more than the net inward current, and thus shortened the ARI to some degree. Propranolol might counteract the adrenergic effects and prolong ARI in the ventricle. Similar results in the QT interval have been observed in patients with LQT3 treated with a beta-adrenergic blocker.[4] However, Head *et al.*[9] showed that the local electrogram duration was increased by propranolol in genetically modified Langendorff-perfused murine hearts modelling LQT3. They also reported that neither isoprenaline nor propranolol had any effect on the arrhythmogenecity in their genetically modified model of LQT3. Therefore, although the precise mechanisms are still uncertain, the effects of adrenergic stimulation in

ventricular repolarization and/or occurrence of polymorphic VA were non-uniform in different models of LQT3.

Epinephrine-induced polymorphic ventricular tachyarrhythmia

Triggered premature activity originating from the Purkinje network or subendocardium and heterogeneity of ventricular repolarization are the two key factors in the initiation and perpetuation of polymorphic VA in LQTS.[26-28] As observed in previous studies with this AP-A model,[17,18] in this study epinephrine-induced polymorphic VA appeared to be preceded by delayed conduction or functional conduction block of the premature wave front at LV Mid and Endo sites (*Figure 2*). Since polymorphic VA developed soon after the administration of epinephrine, the distribution of ventricular repolarization at that time point might not have been sufficiently homogeneous as the result of epinephrine. Indeed, distribution of the transmural ventricular repolarization was heterogeneous at the initiation of polymorphic VA, as shown in *Figure 2*. In our previous studies of the AP-A model of LQT3, large transmural dispersion of ventricular repolarization was not observed in canine hearts before the administration of AP-A.[13,19]

Epinephrine usually shortens the cardiac cycle length and such changes in cardiac cycle can profoundly affect the QT segment of patients with LQTS.[29] Nuyens *et al.*[10] reported that pacing-induced sudden acceleration in the heart rate or premature beats caused transient lengthening of the action potential with early afterdepolarization, and triggered arrhythmia in a genetically modified mice model of LQT3. However, in their study, such paradoxical prolongation of the ventricular repolarization was not observed when the heart rate was progressively accelerated by the administration of isoproterenol. In this study, the cardiac cycle was fixed by RV pacing after the creation of the AV block.

Therapeutic effects of propranolol in this LQT3 model

In this study, inhibition of triggered PVC and a decrease in LV transmural ARI dispersion might have been responsible for the suppression of the epinephrine-induced polymorphic VA by propranolol. The former is suggested to be the more important factor, since epinephrine did not trigger any PVC after the administration of propranolol.

The results of this study support the therapeutic effects of propranolol against arrhythmias in LQT3 syndrome during ventricular pacing at a cycle length of 750 ms. However, the basal pacing rate might determine the effects of epinephrine or propranolol in this model. A slow heart rate seemed to accentuate the heterogeneous distribution of ventricular repolarization and facilitate the induction of PVC by epinephrine.[17,19,23,28] On the other hand, a faster pacing rate should attenuate the heterogeneity of ventricular repolarization and decrease the number of triggered PVC.[17,19,23,28] A relatively short diastolic interval during more rapid pacing potentially influences the myocardial ionic currents (including I_{Ks} and other currents) and modifies the restitution curve of the ventricular repolarization.[19,30,31] It has been reported that characteristics of the restitution curve are associated with the occurrence of VA in LQT2 and LQT3 models.[32,33] Therefore, the effects of epinephrine or propranolol (or both) on the distribution of ventricular repolarization and development of VA may need to be studied in several different ranges of basic pacing cycle length.

Clinical implications

Beta-adrenergic blockade effectively suppressed the epinephrine-induced PVC and polymorphic VA in this LQT3 model. Therefore, beta-adrenergic blockers have potential in small doses as supplemental therapy to suppress episodes of VA in patients suffering from LQT3, preferably combined with a pacemaker or an implantable cardioverter defibrillator to prevent marked bradycardia.

Study limitations

A first limitation of this study was the limited number of needle electrodes used and myocardial areas explored, which might have underestimated the heterogeneity of ventricular repolarization. The steepest repolarization gradients between the surface of the epicardium and the deep subepicardium are difficult to detect with unipolar electrograms that begin at a depth of 0.5 mm. Furthermore, the origin of triggered premature activity and mechanism of the epinephrine-induced polymorphic VA were not identified because of the low resolution of the local electrograms. However, it is likely that the electrophysiological mechanisms of polymorphic VA in this study were the same as those previously observed by detailed mapping in the same experimental model.[17,18] Second, epinephrine augments both beta- and alpha-adrenergic activity, and the role played by beta- vs. alpha-adrenergic activation with respect to the ARI distribution and polymorphic VA was not examined separately. However, in clinical cases, sympathetic nervous activity enhances both alpha- and beta-adrenergic tones, although beta-adrenergic blockers, instead of alpha- and beta-adrenergic blockers together, have been used as a first-line medical treatment of congenital LQTS. Third, complete data from control experiments without AP-A is important to support the results of this study, but these were not performed here. Nevertheless, it seems to be reasonable to think that multiple PVCs and heterogeneous ventricular repolarization are two key factors in the induction of polymorphic VA by epinephrine (1.0 μg/kg) in this model because similar PVCs, but not polymorphic VA, were induced by the same dose of epinephrine before the administration of AP-A. Finally, the animals were anesthetized with thiopental, which might antagonize the increase in late Na^+ current by AP-A.

Conclusions

Epinephrine was demonstrated to have bidirectional effects on ventricular electrical stability, depending on its dosage, in an AP-A model of LQT3. Small doses of epinephrine resulted in homogeneous distribution of the ventricular repolarization, whereas a larger dose induced sustained polymorphic VA. Propranolol prevented the induction of epinephrine-induced polymorphic VA without increasing the heterogeneity of ventricular repolarization during fixed ventricular pacing.

Conflict of interest: none declared.

References

1. Schwartz PJ, Priori SG, Spazzolini C, Moss AJ, Vincent GM, Napolitano C *et al.* Genotype-phenotype correlation in the long QT syndrome. Gene-specific triggers for life-threatening arrhythmias. *Circulation* 2001;**103**: 89-95.
2. Roden DM, Lazzara R, Rosen MR, Schwartz PJ, Towbin J, Vincent GM. Multiple mechanisms in the long QT syndrome: current knowledge, gaps and future directions. *Circulation* 1996;**94**:1996-2012.
3. Schwartz PJ, Locati EH, Moss AJ, Crampton RS, Trazzi R, Ruberti U. Left cardiac sympathetic denervation in the therapy of congenital long QT syndrome. *Circulation* 1991;**84**:503-11.
4. Moss AJ, Zareba W, Hall J, Schwartz PJ, Crampton RS, Benhorin J *et al.* Effectiveness and limitations of β-blocker therapy in congenital long QT syndrome. *Circulation* 2000;**101**:616-23.
5. Priori SG, Napolitano C, Schwartz PJ, Grillo M, Bloise R, Ronchetti E *et al.* Association of long QT syndrome loci and cardiac events among patients treated with β-blockers. *JAMA* 2004;**292**:1341-4.
6. Shimizu W, Antzelevitch C. Differential effects of beta-adrenergic agonists and antagonists in LQT1, LQT2 and LQT3 models of the long QT syndrome. *J Am Coll Cardiol* 2000;**35**:778-86.
7. Priori SG, Napolitano C, Cantu F, Brown AM, Schwartz PJ. Differential response to Na^+ channel blockade, beta-adrenergic stimulation and rapid pacing in a cellular model mimicking the SCN5A and HERG defects present in the long QT syndrome. *Circ Res* 1996;**98**:2314-22.
8. Shimizu W, Antzelevitch C. Cellular basis for the electrocardiographic features of the LQT1 form of the long QT syndrome: effects of β-adrenergic agonists, antagonists and sodium channel blockers on transmural dispersion of repolarization and torsade de pointes. *Circulation* 1998;**98**:2314-22.
9. Head CE, Balasubramaniam R, Thomas G, Goddard CA, Lei M, Colledge WH *et al.* Paced electrogram fractionation analysis of arrhythmogenic tendency in ΔKPQ Scn5a Mice. *J Cardiovasc Electrophysiol* 2005;**16**:1329-40.
10. Nuyens D, Stengl M, Dugarmaa S, Rossenbacker T, Compernolle V, Rudy Y *et al.* Abrupt rate acceleration or premature beats cause life-threatening arrhythmias in mice with long-QT3 syndrome. *Nat Med* 2001;**7**:1021-7.
11. El-Sherif N, Caref EB, Chinushi M, Restivo M. Mechanism of arrhythmogenicity of the short-long cardiac sequence that precedes ventricular tachyarrhythmias in the long QT syndrome. *J Am Coll Cardiol* 1999;**33**: 1415-23.
12. Chinushi M, Hosaka Y, Washizuka T, Furushima H, Aizawa Y. Arrhythmogenesis of T wave alternans associated with surface QRS complex alternans and the role of ventricular prematurity (Observations from a canine model of LQT3 syndrome). *J Cardiovasc Electrophysiol* 2002;**13**: 599-604.
13. Chinushi M, Caref EB, Restivo M, Noll G, Aizawa Y, El-Sherif N. Cycle-length associated modulation of the regional dispersion of ventricular repolarization in a canine model of long QT syndrome. *Pacing Clin Electrophysiol* 2001;**24**:1247-57.
14. Sicouri S, Fish J, Antzelevitch C. Distribution of M cells in the canine ventricle. *J Cardiovasc Electrophysiol* 1994;**5**:824-37.
15. Millar CK, Kralios FA, Lux RL. Correlation between refractory periods and ARIs from electrograms: effects of rate and adrenergic interventions. *Circulation* 1985;**72**:1372-9.
16. Haws CW, Lux RL. Correlation between in vivo transmembrane action potential durations and activation recovery intervals from electrograms: effects of interventions that alter repolarization time. *Circulation* 1991; **81**:281-28.
17. El-Sherif N, Caref EB, Yin H, Restivo M. The electrophysiological mechanism of ventricular tachyarrhythmias in the long QT syndrome: three-dimensional mapping of activation and recovery patterns. *Circ Res* 1996;**79**:474-92.
18. El-Sherif N, Chinushi M, Caref EB, Restivo M. Electrophysiological mechanism of the characteristic electrocardiographic morphology of torsade de pointes tachyarrhythmias in the long QT syndrome. *Circulation* 1997;**96**:4392-9.
19. Chinushi M, Restivo M, Caref EB, El-Sherif N. The electrophysiological basis of arrhythmogenecity of QT/T alternans in long QT syndrome. Tridimentional analysis of the kinetics of cardiac repolarization. *Circ Res* 1998;**83**:614-28.
20. Zygmunt AC. Intracellular calcium activates chloride current in canine ventricular myocytes. *Am J Physiol* 1994;**267**:H1984-95.
21. Zygmunt AC, Goodrow RJ, Antzelevitch C. INaCa contributes to electrical heterogeneity within the canine ventricle. *Am J Physiol Heart Circ Physiol* 2000;**278**:H1671-67.
22. Liu DW, Antzelevitch C. Characteristics of the delayed rectifier current (Ikr and Iks) in canine ventricular epicardial, midmyocardial, and endocardial myocytes: a weaker Iks contributes to the longer action potential of the M cell. *Circ Res* 1995;**76**:351-65.
23. Shimizu W, Noda T, Takaki H, Nagaya N, Satomi K, Kurita T *et al.* Diagnostic value of epinephrine test for genotyping LQT1, LQT2, and LQT3 forms of congenital long QT syndrome. *Heart Rhythm* 2004;**1**:276-83.
24. Zygmunt AC, Eddlestone GT, Thomas GP, Nesterenko VV, Antzelevitch C. Larger late sodium conductance in M cells contributes to electrical heterogeneity in canine ventricle. *Am J Physiol Heart Circ Physiol* 2001; **281**:H689-97.
25. Yan GX, Shimizu W, Antzelevitch C. Characteristics and distribution of M cells in arterially perfused canine left ventricular wedge preparations. *Circulation* 1998;**98**:1921-7.
26. Restiovo M, Caref EB, Kozhevnikov DO, El-Sherif N. Spatial dispersion of repolarization is a key factor in the arrhythmogenicity of long QT syndrome. *J Cardiovasc Electrophysiol* 2004;**15**:323-31.
27. Surawicz B. Electrophysiological substrate of torsade de pointes: dispersion of repolarization or early afterdepolarizations? *J Am Coll Cardiol* 1989;**14**:172-84.
28. Shimizu W, Aiba T, Antzelevitch C. Specific therapy based on the genotype and cellular mechanism in inherited cardiac arrhythmias. Long QT syndrome and Brugada syndrome. *Curr Pharm Des* 2005;**11**:1561-72.
29. Viskin S, Rosso R, Rogowski O, Belhassen B, Levitas A, Wagshal A *et al.* Provocation of sudden heart rate oscillation with adenosine exposes abnormal QT response in patients with long QT syndrome: a bedside test for diagnosing long QT syndrome. *Eur Heart J* 2006;**27**:469-75.
30. Boyett MR, Jewell BR. A study of the factors responsible for rate-dependent shortening of the action potential in mammalian ventricular muscle. *J Physiol (Lond)* 1978;**285**:359-80.
31. Riccio ML, Koller ML, Gilmour RF Jr. Electrical restitution and spatiotemporal organization during ventricular fibrillation. *Circ Res* 1999;**84**: 955-63.
32. Yamauchi S, Yamaki M, Watanabe T, Yuuki K, Kubota I, Tomoike H. Restitution properties and occurrence of ventricular arrhythmia in LQT2 type of Long QT syndrome. *J Cardiovasc Electrophysiol* 2002;**13**:910-4.
33. Sabir IN, Li LM, Jones VJ, Goddard CA, Grace AA, Huang C L-H. Criteria for arrhythmogenicity in genetically-modified Langendorff-perfused murine hearts modeling the congenital long QT syndrome type 3 and the Brugada syndrome. *Pflugers Arch* 2008;**455**:637-51. Epub September 6, 2007.

Journal of the American College of Cardiology
© 2007 by the American College of Cardiology Foundation
Published by Elsevier Inc.

Vol. 50, No. 18, 2007
ISSN 0735-1097/07/$32.00

CORRESPONDENCE

Research Correspondence

Anti-KCNH2 Antibody-Induced Long QT Syndrome

Novel Acquired Form of Long QT Syndrome

To the Editor: The acquired form of long QT syndrome (LQTS) is often induced by hypokalemia or drugs. Hypokalemia and drugs cause QT prolongation via reduction in the rapidly activating component of the delayed rectifier K^+ currents (I_{Kr}). Therefore, the KCNH2 (HERG) channel conducting I_{Kr} is recognized as the most susceptible channel in acquired LQTS. However, the autoimmune effect on the KCNH2 channel has not been elucidated.

In the present report, we describe a female patient with an acquired form of LQTS with no known cause of QT prolongation. We used the patch clamp method (1) to determine whether her serum and immunoglobulin (Ig)G reduced I_{Kr}, and we performed Western blot analysis to determine whether her IgG included anti-KCNH2 antibodies.

The patient was a 42-year-old female who had a normal clinical history until recurrent episodes of syncope for 3 months. An electrocardiogram (ECG) showed marked QT prolongation, T-wave alternans, and episodes of Torsades de pointes (Fig. 1A). Treatment with atrial pacing (70/min) and intravenous magnesium infusion were started, but the corrected QT interval (QTc) was persistently prolonged (0.70 $s^{0.5}$) (Fig. 1B). The ECGs obtained at annual checkups for the previous 4 years were normal or at most borderline (0.45 to 0.46 for women), but with normal T-wave morphology and not suggestive of LQTS (QTc 0.43 $s^{0.5}$) (Fig. 1C), and there was no family history of QT prolongation or cardiac sudden death. The patient was not taking any drugs, and there was no evidence of structural heart disease or cerebrovascular disease. Laboratory data, including serum electrolytes and hormones, were normal except for detection of increased IgG concentration (1,783 mg/dl) and positive anti-Sjögren's syndrome A (SSA)/Ro antibodies (141.3 index). The recurrence of syncope was diminished by oral administration of atenolol (100 mg/day) and verapamil (120 mg/day). The patient was discharged after implantation of an implantable cardioverter-defibrillator with pacing mode DDI (lower: 70/min). Prolonged QT interval and increased IgG level have remained, but ventricular tachycardia or fibrillation events have not been detected.

We screened for known LQTS-associated genes by polymerase chain reaction DNA conformation polymorphism analysis and DNA sequencing. We suspected LQT2 because of low-amplitude T waves in the ECG, but there was no mutation in the *KCNH2* gene. Furthermore, no mutation was detected in *KCNQ1*, *SCN5A*, *KCNE1*, *KCNE2*, and *KCNJ2* genes. There was a polymorphism (D85N) in *KCNE1*, which is heterozygously found in 2% of the Japanese population. Because ECGs for the previous 4 years were normal, D85N-*KCNE1* may have not a causative but rather a modifying role in this LQTS patient.

The KCNH2 current stably expressed in HEK 293 cells was significantly reduced when cells had been cultured for 1 to 5 days in a medium to which 2% serum from the patient (Figs. 2A and 2D) or IgG (75 μg/ml) (Figs. 2B to 2D) had been added. When cells expressing KCNH2 that had been cultured in the patient's serum were returned to the medium without serum overnight, the amplitudes of both KCNH2 outward and tail currents recovered to untreated levels. The patient's serum had no effect on the slowly activating components of the delayed rectifier K^+ currents (I_{Ks}) of HEK 293 cells expressing KCNQ1/KCNE1 (data not shown). Next, we tested whether the patient's serum has an acute effect on KCNH2 currents (I). Direct application of 2% serum from the patient to physiologic solution for 5 min had no effect on either I_{step} or I_{tail}. These findings suggest that the patient's IgG decreased KCNH2 expression. The mechanism is not clear, but endocytosis may be facilitated.

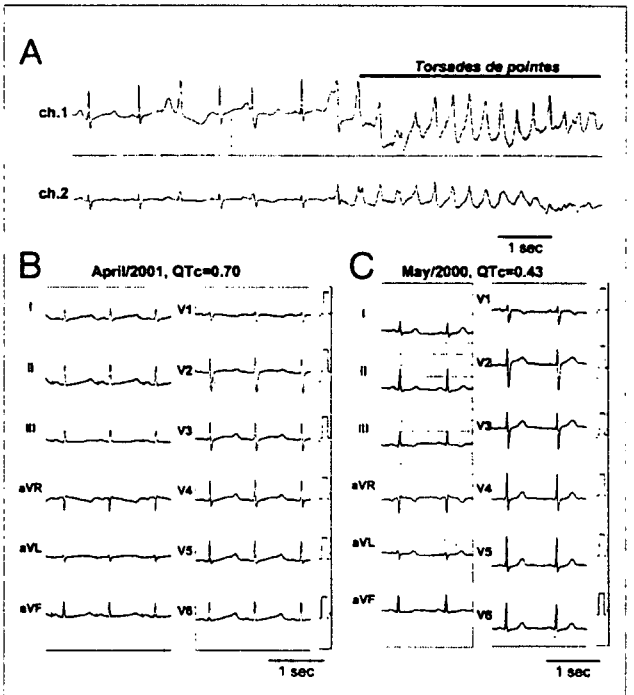

Figure 1 **Electrocardiogram Traces of a Patient With Acquired QT Prolongation**

(A) Marked QT prolongation and Torsades de pointes shown in 24-h electrocardiogram traces. **(B)** Prolonged QT interval was persistently observed after the initial episodes (corrected QT interval [QTc] 0.70 $s^{0.5}$). **(C)** Twelve-lead electrocardiogram 1 year before is normal (QTc 0.43 $s^{0.5}$).

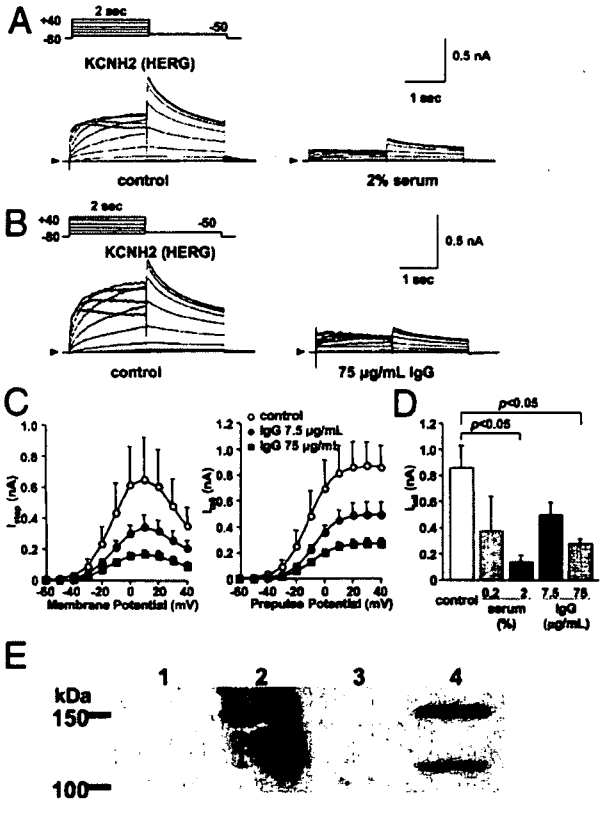

Figure 2 **KCNH2 (HERG) Channel Currents and Western Blot Analysis of Autoantibodies Produced Against KCNH2**

(A) Representative KCNH2 (HERG) channel currents recorded from HEK 293 cells cultured in control medium **(left)** and medium supplemented with 2% serum from the patient **(right)**. **(B)** Representative KCNH2 channel currents recorded from HEK 293 cells cultured in control medium **(left)** and medium supplemented with 75 μg/ml immunoglobulin (Ig)G from the patient **(right)**. **(C)** Current (I)–voltage relationships of I_{step} **(left)** and I_{tail} **(right)** recorded from HEK 293 cells cultured in control medium (**open circles**; n = 4) or a medium supplemented with either 7.5 μg/ml (**solid circles**; n = 7) or 75 μg/ml (**solid squares**; n = 7) IgG. The lines fitted to I_{tail} data **(right)** represent Boltzmann functions. **(D)** A comparison of the dose-dependent effects of serum (0.2% and 2%) and IgG (7.5 and 75 μg/ml) added to the culture medium (control) of HEK 293 cells expressing KCNH2 on maximal I_{tail} amplitude. **(E)** Western blot analysis of autoantibodies produced against KCNH2. **Lane 1**: IgG from a healthy control subject; **lane 2**: IgG from the patient; **lane 3**: pre-incubation of the HEK 293 lysate expressing KCNH2 protein with IgG from the patient; **lane 4**: anti-KCNH2 polyclonal antibodies (positive control).

In Western blotting of the lysate of HEK 293 cells expressing KCNH2, no band was detected in the presence of IgG from a healthy control subject (Fig. 2E, lane 1). A single distinct band of approximately 150 kDa was evident in the presence of IgG from the patient (Fig. 2E, lane 2). This band was absorbed by preincubation with the lysate of HEK 293 cells expressing KCNH2 protein (Fig. 2E, lane 3). A band of the same size was recognized in the presence of rabbit antiHERG polyclonal antibodies (Alomone Labs, Jerusalem, Israel) (Fig. 2E, lane 4). A 155-kDa (upper) band is a mature form of the KCNH2 channel and a 135-kDa (lower) band is a precursor form of the KCNH2 channel (2). Figure 2B shows the upper band in the presence of the patient's IgG. Therefore, the patient's IgG contains autoantibodies against the mature form of KCNH2 protein.

Cross-reaction of anti-SSA/Ro antibodies with the L-type calcium channel has been reported (3). Lazzerini et al. (4) have also reported that patients with anti-SSA/Ro–positive connective tissue diseases show a high prevalence of QTc prolongation. In the present study, the patient had positive anti-SSA/Ro antibodies. Cross-reaction of anti-SSA/Ro antibodies with the KCNH2 channel may be involved in the pathogenesis of autoimmunity. Immunosuppressive therapy and reduction of plasma IgG may be effective for QT-interval shortening in the future. Further studies are needed to clarify this point.

In summary, our results show that abnormal IgG from a patient with acquired LQTS reduces the KCNH2 current and that the IgG includes anti-KCNH2 antibody. This is the first report of anti-KCNH2 antibody-induced LQTS.

***Kazufumi Nakamura, MD, PhD**

*Department of Cardiovascular Medicine
Okayama University Graduate School of Medicine, Dentistry, and Pharmaceutical Sciences
2-5-1 Shikata-cho
Okayama 700-8558
Japan
E-mail: ichibun@cc.okayama-u.ac.jp

Yusuke Katayama, MD, PhD
Kengo F. Kusano, MD, PhD
Kayo Haraoka, MD
Yoshinori Tani, MD
Satoshi Nagase, MD, PhD
Hiroshi Morita, MD, PhD
Daiji Miura, PhD
Yoshihisa Fujimoto, MD, PhD
Tetsushi Furukawa, MD, PhD
Kazuo Ueda, MD
Yoshiyasu Aizawa, MD
Akinori Kimura, MD, PhD
Yoshihisa Kurachi, MD, PhD
Tohru Ohe, MD, PhD, FACC

doi:10.1016/j.jacc.2007.07.037

Please note: Drs. Nakamura and Katayama contributed equally to this work.

REFERENCES

1. Katayama Y, Fujita A, Ohe T, Findlay I, Kurachi Y. Inhibitory effects of vesnarinone on cloned cardiac delayed rectifier K(+) channels expressed in a mammalian cell line. J Pharmacol Exp Ther 2000;294: 339–46.
2. Zhou Z, Gong Q, Epstein ML, January CT. HERG channel dysfunction in human long QT syndrome. Intracellular transport and functional defects. J Biol Chem 1998;273:21061–6.
3. Xiao GQ, Qu Y, Hu K, Boutjdir M. Down-regulation of L-type calcium channel in pups born to 52 kDa SSA/Ro immunized rabbits. FASEB J 2001;15:1539–45.
4. Lazzerini PE, Acampa M, Guideri F, et al. Prolongation of the corrected QT interval in adult patients with antiRo/SSA-positive connective tissue diseases. Arthritis Rheum 2004;50:1248–52.

Available online at www.sciencedirect.com
ScienceDirect
Journal of Molecular and Cellular Cardiology 43 (2007) 187–196
Journal of Molecular and Cellular Cardiology
www.elsevier.com/locate/yjmcc

Original article

T75M-KCNJ2 mutation causing Andersen–Tawil syndrome enhances inward rectification by changing Mg^{2+} sensitivity

Yoshinori Tani [a,b], Daiji Miura [b], Junko Kurokawa [a], Kazufumi Nakamura [b], Mamoru Ouchida [c], Kenji Shimizu [c], Tohru Ohe [b], Tetsushi Furukawa [a,*]

[a] *Department of Bio-Informational Pharmacology, Medical Research Institute, Tokyo Medical and Dental University, 2-3-10 Kandasurugadai, Chiyoda-ku, Tokyo 101-0062, Japan*
[b] *Department of Cardiovascular Medicine, Okayama Univeristy Graduate, School of Medicine, Dentistry and Pharmaceutical, Sciences, Okayama, Japan*
[c] *Department of Molecular Genetics, Okayama University Graduate School of Medicine, Dentistry and Pharmaceutical, Sciences, Okayama, Japan*

Received 30 November 2006; received in revised form 4 April 2007; accepted 4 May 2007
Available online 18 May 2007

Abstract

Andersen–Tawil syndrome (ATS) is a multisystem inherited disease exhibiting periodic paralysis, cardiac arrhythmias, and dysmorphic features. In this study, we characterized the KCNJ2 channels with an ATS mutation (T75M) which is associated with cardiac phenotypes of bi-directional ventricular tachycardia, syncope, and QT_c prolongation. Confocal imaging of GFP-KCNJ2 fusion proteins showed that the T75M mutation impaired membrane localization of the channel protein, which was restored by co-expression of WT channels with T75M channels. Whole-cell patch-clamp experiments in CHO-K1 cells showed that the T75M mutation produced a loss-of-function of the channel. When both WT and the T75M were co-expressed, the T75M mutation showed dominant-negative effects on inward rectifier K^+ current densities, with prominent suppression of outward currents at potentials between 0 mV and +80 mV over the E_K. Inside-out patch experiments in HEK293T cells revealed that co-expression of WT and the T75M channels enhanced voltage-dependent block of the channels by internal Mg^{2+}, resulting in enhanced inward rectification at potentials 50 mV more positive than the E_K. We suggest that the T75M mutation causes dominant-negative suppression of the co-expressed WT KCNJ2 channels. In addition, the T75M mutation caused alteration of gating kinetics of the mutated KCNJ2 channels, i.e., increased sensitivity to intracellular Mg^{2+} and resultant enhancement of inward rectification. The data presented suggest that the mutation may influence clinical features, but it does not directly show this.

Keywords: Andersen–Tawil syndrome; QT_c prolongation; KCNJ2; The Kir2.1 (I_{K1}) channel; Inward rectification; Magnesium; Spermine

1. Introduction

Andersen–Tawil syndrome (ATS) is a heterogeneous multi-system disease, and typically presents the triad of periodic paralysis, cardiac arrhythmias, and dysmorphic features [1,2]. ATS occurs in an autosomal-dominant inheritance or sporadically. In either case, mutations in the locus of chromosome 17q23.1–q24.2 of the gene *KCNJ2* have been reported [3–11]. *KCNJ2* encodes the inwardly rectifying K^+ channel, Kir2.1 [12], which contributes to excitability of heart, brain, and skeletal muscle [13]. In heart, Kir2.1 is the main α subunit of I_{K1}, a current which stabilizes resting membrane potential and regulates late phase 3 repolarization of the cardiac action potential [14]. In ATS patients, suppression of I_{K1} brought about by *KCNJ2* mutation can destabilize resting membrane

Abbreviations: ATS, Andersen–Tawil syndrome; GFP, green fluorescent protein; WT, wild type; CHO-K1 cell, Chinese hamster ovary-K1 cell; HEK293T cell, human embryonic kidney 293T cells; E_K, potassium reversal potential; I_{K1}, inward rectifying potassium current; PIP_2, phosphatidylinositol 4,5-diphosphate; ECG, electrocardiogram; PCR, polymerase chain reaction; cDNA, complementary deoxyribonucleic acid; PBS, phosphate buffered saline; HEPES, 2-[4-(2-hydroxyethyl)-1-piperadinyl] ethansulfonic acid; ATP, adenosine triphosphate; *I–V*, current to voltage; NMDG-Cl, *N*-methyl-D-glucamine chloride; EDTA, ethylenediaminetetracetic acid; S.E.M., standard error of mean; ANOVA, analysis of variance; Thr, threonine; Met, methionine; C, cytosine; T, thymine; Glu, glutamic acid; Asp, aspartic acid; Asn, asparagine; LQT, long QT syndrome; SQT, short QT syndrome.

* Corresponding author. Tel.: +81 3 5280 8070; fax: +81 3 5280 8071.
E-mail address: t_furukawa.bip@mri.tmd.ac.jp (T. Furukawa).

0022-2828/$ - see front matter © 2007 Elsevier Inc. All rights reserved.
doi:10.1016/j.yjmcc.2007.05.005

potential and, in some cases, can cause prolongation of QT_c intervals, resulting in a heightened propensity for arrhythmias.

There are currently more than 20 mutations identified in ATS patients in distinct regions of *KCNJ2*. Most of ATS mutations in *KCNJ2* cause reduction of the Kir2.1 channel activity in a loss-of-function or a dominant-negative fashion. Some ATS mutations are attributable to defective trafficking of channel proteins to the plasma membrane [8,10], whilé others reflect decreased affinity for PIP_2 [6]. However, the mechanisms underlying many of the mutations which alter Kir2.1 channel function remain unclear.

In a Japanese family of ATS with clinical features of bi-directional ventricular tachycardia, prolonged QT_c interval, and syncope, we identified a T75M *KCNJ2* mutation at the amino-terminus of the Kir2.1 channel. In recombinant expression systems, we found that this mutation has a dominant-negative effect on the Kir2.1 channel function; interestingly, the hetero-multimeric channel composed of WT and the T75M mutant Kir2.1 showed increased sensitivity to voltage-dependent block by intracellular Mg^{2+}, resulting in prominent reduction in outward component of I_{K1} and enhanced inward rectification.

2. Methods

2.1. Clinical description

A 35-year-old female was referred to Okayama University hospital for evaluation of syncope associated with bi-directional ventricular tachycardia (Fig. 1B). She is short (140.0 cm; 39.1 kg), has never experienced episodes of periodical paralysis, and her serum K^+ level was within normal range (4.1–4.3 mEq/L). In Fig. 1A, a resting 12-lead ECG shows a prolonged QT_c interval (red bars in Fig. 1A; $QT_c = 0.50$ s) with a prominent U wave (arrows in Fig. 1A). An exercise stress test augmented the incidence of non-sustained polymorphic ventricular tachycardias. No obvious organic heart disease was found by cardiac evaluation including echocardiography, cardiac scintigraphy, cardiac magnetic resonance imaging, coronary arteriography, left and right ventriculography, and cardiac biopsy. A β-blocker, Ia or Ic antiarrhythmic drugs were ineffective for ventricular arrhythmias. Her daughter (15-year-old) is also short (141.2 cm; 37.1 kg), and exhibited multifocal premature ventricular contractions ($QT_c = 0.44$ s).

2.2. DNA extraction and mutation analysis

This study complied with the Guidelines for Human Genome Studies Ethics Committee of Okayama University; informed consent was obtained. Genomic DNA was extracted from peripheral blood leukocytes by using DNA extraction kit (Gentra, USA), and was stored at −30 °C until use. We carried out PCR using leukocyte genomic DNA as a template. The entire region of exon 2 of the *KCNJ2* was amplified with 5 sets of oligonucleotide primers as described by Hosaka et al. [5]. PCR products were directly sequenced with the ABI Prism 3130xl Genetic Analyzer (Applied Biosystems, Foster city, USA) by using BigDye Terminator Sequencing Standard Kit (Ver. 1.1, Applied Biosystem, USA).

2.3. Expression plasmids

The entire coding region of the *KCNJ2* was amplified from genomic DNA of the patient's leukocytes that contains both WT and mutant (T75M) gene by PCR, using a sense primer S1; 5′-AGCAGAAGCGATGGGCAGTGT and an antisense primer AS1; 5′-CAGTCAGTCATATCTCCGACTC. The PCR products were subcloned into pBluescript KS(−) at *Eco*RV site. For whole-cell patch-clamp assay, the KCNJ2-pBluescript KS(−) was digested with *Sal*I and *Bam*HI, and then was subcloned into pIRES2-EGFP plasmids to prepare pIRES2-EGFP-KCNJ2 (WT) and pIRES2-EGFP-KCNJ2(T75M) [5]. To analyze intracellular localization of the Kir2.1 channel, we constructed a GFP fusion protein of KCNJ2 (GFP-KCNJ2(WT) and GFP-KCNJ2(T75M)): we amplified the *KCNJ2* gene with the sense primer S1 and an antisense primer AS2; 5′-ACGGATCCGA-TATCTCCGACTCTCGCCG to remove the stop codon. The PCR products were digested with *Xho*I and *Bam*HI, and were subcloned into pEGFP-N1. For inside-out patch experiments, cDNAs for WT and mutant KCNJ2 were subcloned into the pCXN2-SK expression vector [15] at *Not*I and *Xho*I sites (pCXN2-KCNJ2(WT) and pCXN2-KCNJ2(T75M)). Sequences of all constructs were verified by DNA sequencing with the ABI3100xl Genetic Analyzer.

2.4. Cell culture and transfection

HEK293T cells (ATCC) were cultured in Dulbecco's modified Eagle's medium (Gibco), and CHO-K1 cells (Riken, Japan) were maintained in Ham's F12 medium. For analyzing intracellular localization of channel protein in Fig. 2, cells were transiently transfected with 0.5 μg GFP-KCNJ2(WT), 0.5 μg GFP-KCNJ2(T75M) or a mixture of 0.5 μg pcDNA3.1-KCNJ2 (WT) and 0.5 μg GFP-KCNJ2(T75M) using Lipofectamine Reagent and Plus Reagent (Invitrogen), as reported previously [16]. For whole-cell experiments (Figs. 3 and 4), cells were transiently transfected with 0.5 μg pIRES2-EGFP-KCNJ2 (WT), pIRES2-EGFP-KCNJ2(T75M), or a mixture of 0.5 μg pIRES-EGFP-KCNJ2(WT) and 0.5 μg pIRES-EGFP-KCNJ2 (T75M). For inside-out patch-clamp experiments (Figs. 5 and 6), cells were transfected with 1 μg pCXN2-KCNJ2(WT) alone or a mixture of 1 μg pCXN2-KCNJ2(WT) and 1 μg pCXN2-KCNJ2(T75M); in both cases, 0.13–0.25 μg pIRES2-EGFP was co-transfected as a transfection marker. Transfected cells were plated on 35-mm petri-dishes unless otherwise noted, and the cells were cultured in a moist 5% CO_2 incubator until use. Experiments were done 48 h after transfection.

2.5. Imaging of the GFP-channel fusion proteins

HEK293T cells transfected with the GFP-fusion Kir2.1 channel genes were cultured in 0.05% poly-L-lysine coated 4-well chamber slides (Iwaki, Japan) to achieve cell attachment. Cells were then fixed with 4% paraformaldehyde, rinsed with

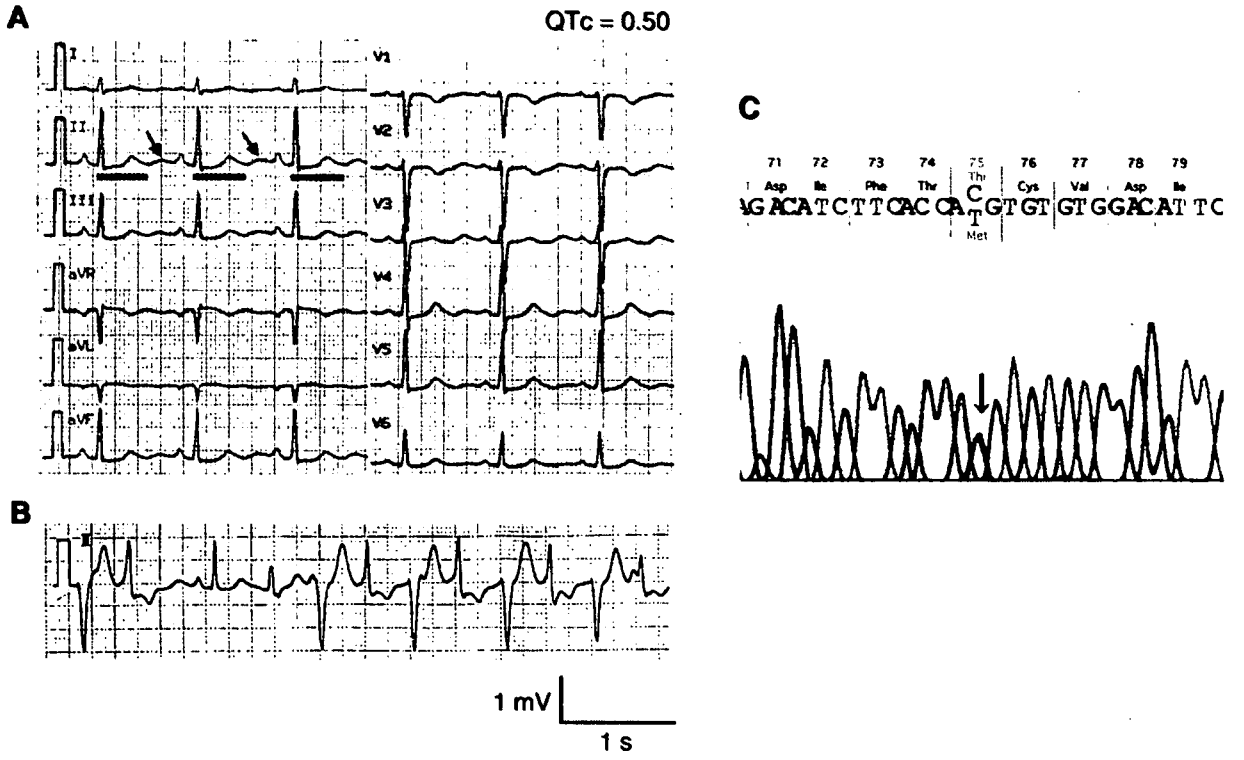

Fig. 1. Identification of *KCNJ2* mutation (T75M) in a Japanese family with ATS. (A) Twelve-lead surface ECG in the proband, 35-year-old female T75M carrier, with a QT_c of 0.5 s. QT intervals are shown by red bars in lead II. The T wave is followed by a prominent U wave (arrows in lead II). (B) Bidirectional ventricular tachycardias in the proband (lead II). (C) Sequence chromatographs of the relevant region of exon 2 of *KCNJ2*. The forward sequence of the proband is shown. The sequence reveals a C and T at nucleotide 224, indicating the normal and mutated sequence, respectively (arrow). This shows that patient is heterozygote for the T75M mutation.

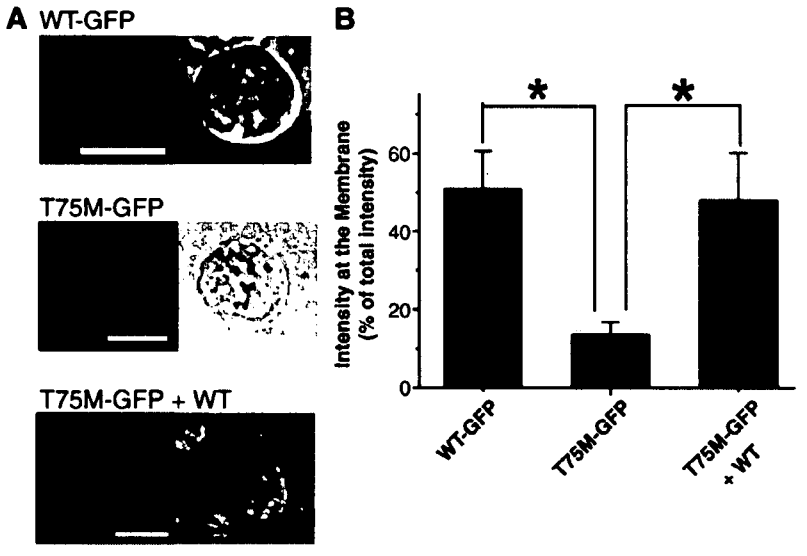

Fig. 2. Impairment of membrane localization by the T75M mutation. (A) Confocal images of HEK293T cells transiently transfected with WT-KCNJ2-GFP (WT-GFP, upper), T75M-KCNJ2-GFP (T75M-GFP, middle), and T75M-KCNJ2-GFP+GFP-unfused WT-KCNJ2 (T75M-GFP/WT, lower). KCNJ2 channels were tagged with GFP at the amino-terminal end, and then location of the GFP-fused channel protein was observed under a confocal microscope (left). Transmitted light images in the same area are shown (right). Scale bars = 10 μm. (B) Summary of the membrane localizations. Shown are percentages of total pixel intensities distributed in 1 μm widths of peripheral regions. Total intensity is obtained from pixel intensity on a line from an edge to another edge of the cell that does not include nuclei. Co-expression of WT (no GFP-tag) restored trafficking impairment of the T75M-GFP channels. Numbers of cells are as follows: WT-GFP $n=6$, T75M-GFP $n=10$, T75M-GFP/WT $n=7$. $^*P<0.05$.

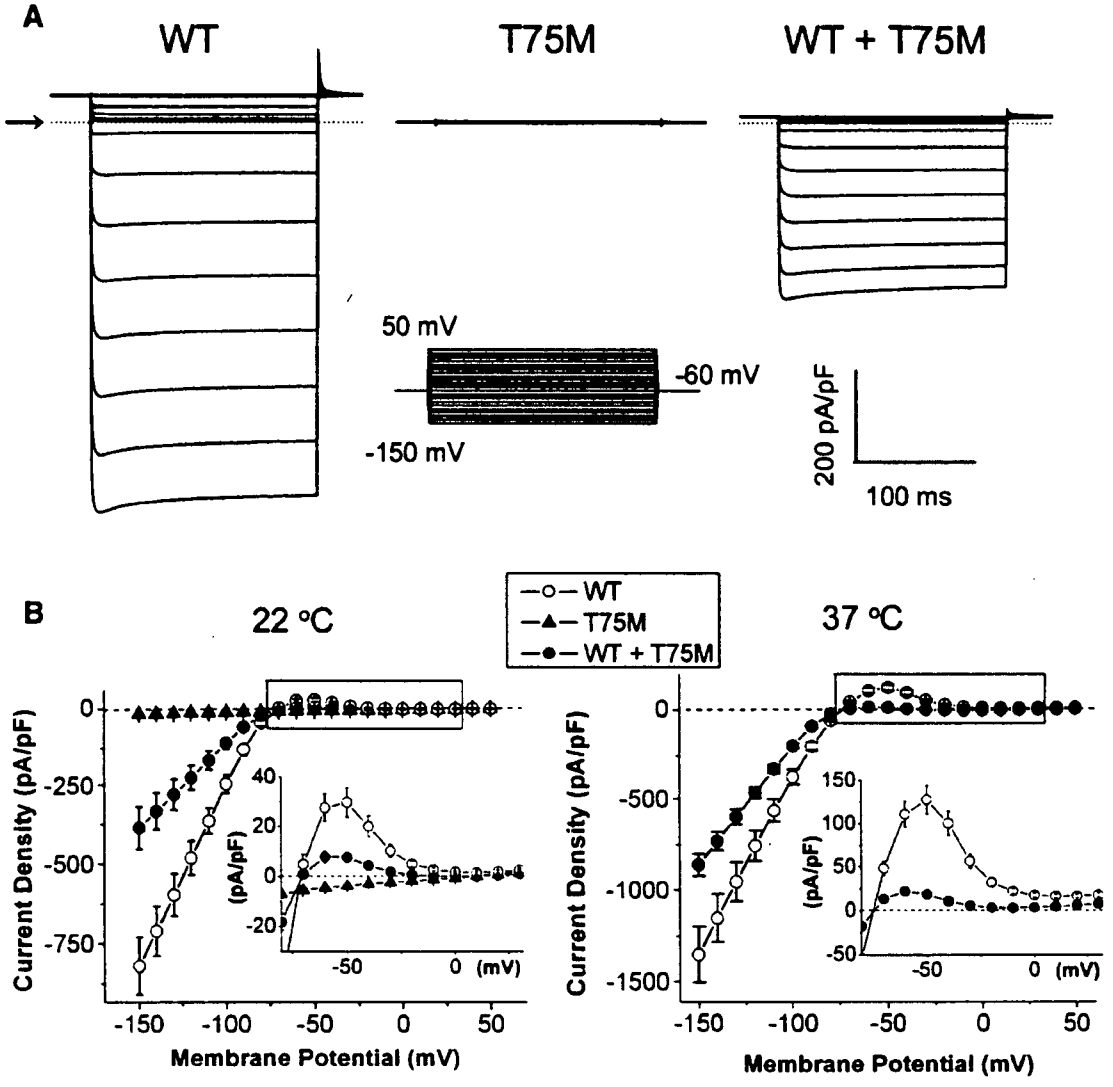

Fig. 3. Dominant-negative effects of the T75M mutation. (A) Representative Kir2.1 current traces recorded in the whole-cell patch-clamp configuration from CHO-K1 cells expressing WT *KCNJ2* (left), T75M (center), and WT/T75M (1:1) at 22 °C. Currents were elicited by test pulses (inset) as described in Methods. Dotted lines show zero-current levels. Scale: 200 pA/pF and 100 ms. (B) Comparison of *I–V* relationships for WT *KCNJ2* (open circles), T75M (closed triangles), and WT/T75M (1:1; closed circles). Experiments were performed either at 22 °C (left, for WT, T75M and WT/T75M) or 37 °C (right, for WT and WT/T75M). Shown are plots of mean instantaneous peak current±SEM vs. pulse voltage as in panel A. Data for statistical analysis were from experiments with CHO-K1 cells prepared on the same day ($n=11$ to 16 for each group). Detectable K^+ currents were not observed from cells transfected with T75M mutant *KCNJ2* alone *(left, closed triangle)*. The T75M *KCNJ2* mutation significantly decreased Kir2.1 currents at most voltages in a dominant-negative manner when co-expressed with WT *KCNJ2* either at 22 °C or at 37 °C. Insets show enlarged plots from −70 mV to +30 mV to emphasize the outward currents without normalization (square in the entire *I–V* plots).

PBS, and then coverslips were mounted onto the slides along with Vecta-shield mounting medium (Vector). Cells were viewed using a Zeiss LSM510 confocal laser-scanning microscope with an ×100 oil-immersion objective lens. GFP was excited with a 488-nm argon laser beam, and fluorescent emission was measured at 505–520 nm. Images were optimized by adjustment of the photo multiplier gain to use the full linear range of pixel intensity, and were averaged from 16-scanning images.

2.6. Electrophysiology

Current recordings were carried out using either the whole-cell patch-clamp technique or the inside-out patch-clamp technique with an Axopatch-1D amplifier (Axon Instruments) as described previously [17]. Signals were low-pass filtered at 2 kHz, sampled at 1 kHz, and compensated for cell capacitance. Series resistance was not compensated. No correction for the liquid junction potential was made. Cells soaked with the bath solution were placed on the stage of an inverted fluorescence microscope (IMT2, Olympus). Expression of the channels was identified visually by viewing GFP fluorescence with a Xenon lamp (Olympus) and an appropriate filter-dichroic set for GFP (Omega Optical). Most of measurements were made at 22± 2 °C: in some experiments, we used temperature at 37±2 °C to examine temperature-dependent effects of T75M mutation on inward rectifying properties of KCNJ2 channels.

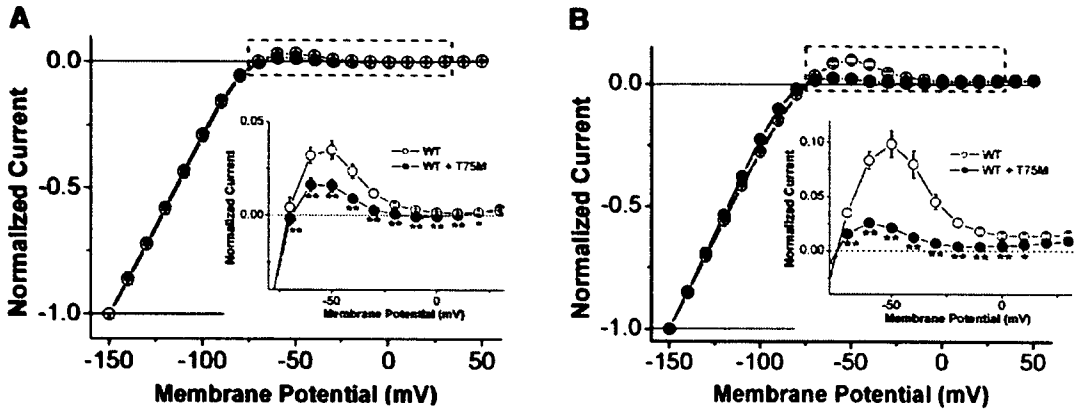

Fig. 4. Enhanced inward rectification of Kir2.1 currents by co-expression with WT and T75M *KCNJ2*. The whole-cell data obtained in Fig. 3B were normalized to the values at −150 mV for each construct (open symbols for WT *KCNJ2*; closed symbols for WT/T75M *KCNJ2*) either at 22 °C (A) or at 37 °C (B). In insets, plots from −70 mV to +30 mV were enlarged to emphasize the outward currents (dotted square in the entire *I–V* plot). The T75M mutation preferentially decreased outward components of the normalized currents, exerting enhanced inward rectification. $*P<0.05$; $**P<0.01$; vs. WT.

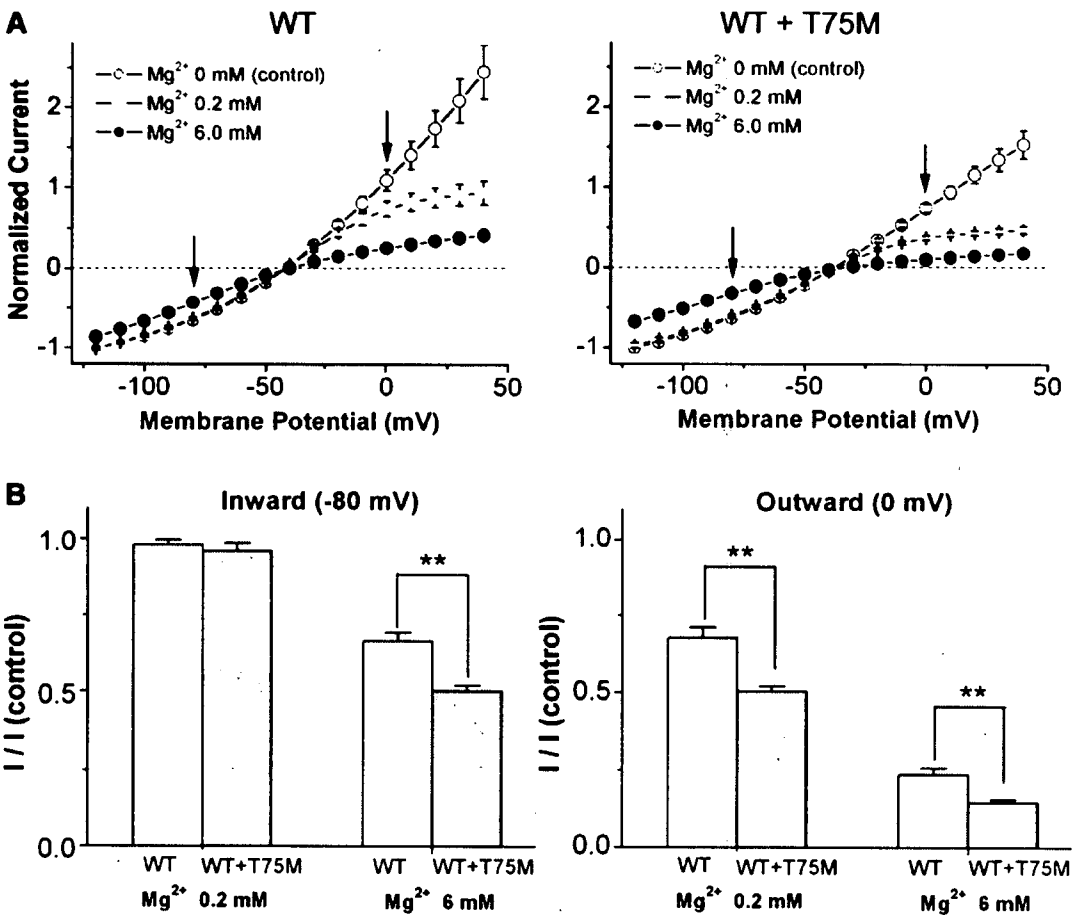

Fig. 5. Enhanced sensitivities to intracellular Mg^{2+} blockade by the T75M mutation. (A) *I–V* relationships. Macroscopic currents were recorded from excised patches of HEK293T cells for WT ($n=6$, left panel) and WT/T75M KCNJ2 ($n=6$, right panel). Currents were elicited by test pulses between −120 mV and +40 mV from a holding potential of −50 mV in 10-mV increments. Intracellular Mg^{2+} (0.2 mM; gray, 6 mM; black) were applied for each patch after washing out of endogenous rectifying molecules (white). Values of amplitudes were plotted relative to those at −120 mV without Mg^{2+} (0 mM, control). (B) Comparison of Mg^{2+} sensitivity between WT (white bars) and WT/T75M KCNJ2 (gray bars) at −80 mV (left panel) and 0 mV (right panel). Bars are mean ratios±SEM of current amplitudes at 0.2 mM Mg^{2+} and 6 mM Mg^{2+}, respectively, being normalized to current amplitudes without Mg^{2+} (control). Normalized values were calculated from data in panel A ($n=6$ for each group). At 0.2 mM Mg^{2+} (at a physiological concentration), the T75M mutation significantly enhanced Mg^{2+}-blockade of only K^+ efflux (outward, 0 mV). At 6 mM Mg^{2+}, the T75M mutation significantly enhanced Mg^{2+}-blockade of both K^+ influx and K^+ efflux. $**P<0.01$; WT vs. WT/T75M.

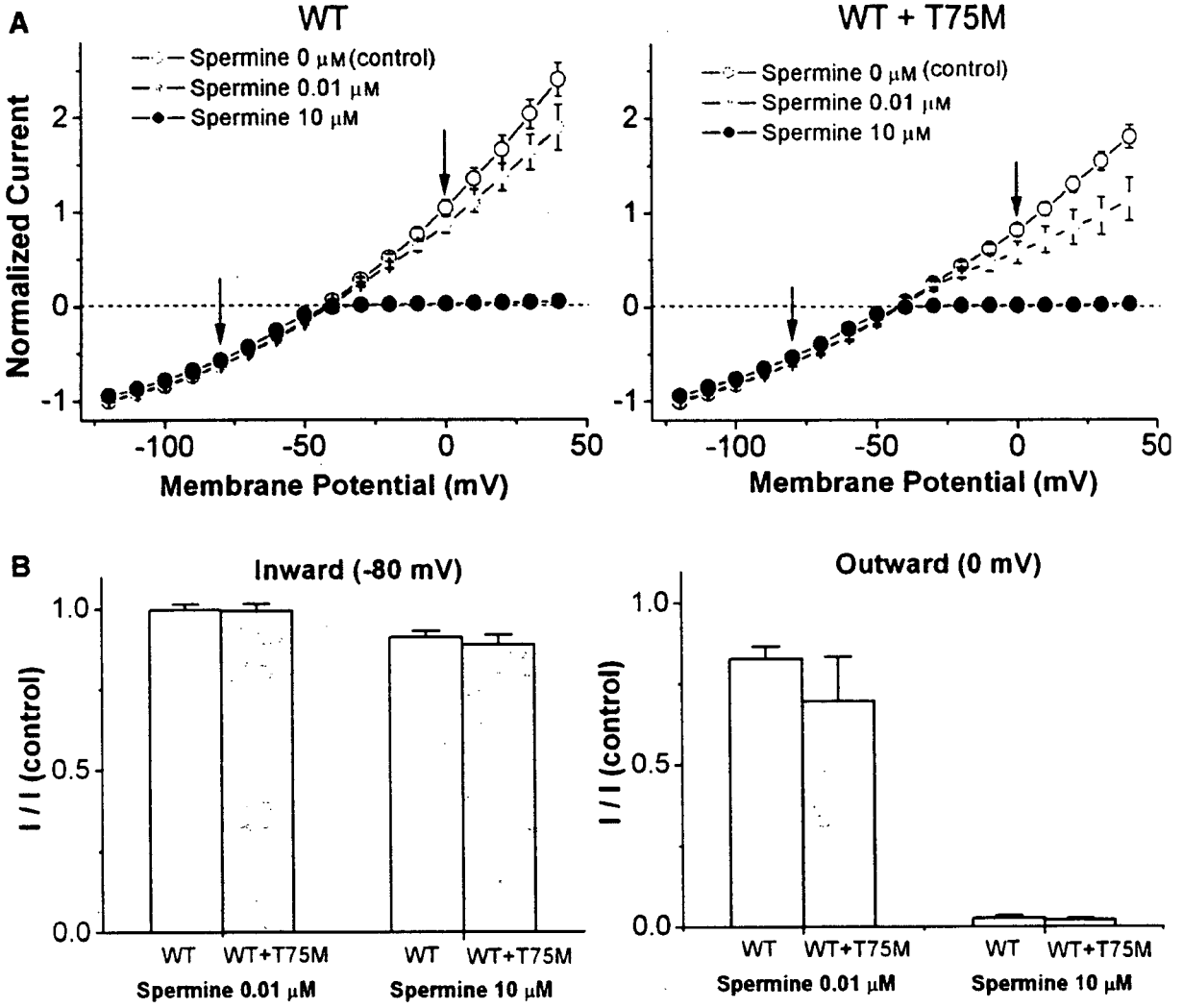

Fig. 6. No change in sensitivities to intracellular spermine-blockade by the T75M mutation. (A) *I–V* relationships. Macroscopic currents were recorded from excised patches of HEK293T cells for WT ($n=6$, left panel) and WT/T75M KCNJ2 ($n=6$, right panel). Currents were measured, and plots are shown, as we described in Fig. 5A. Intracellular spermines (0.01 μM; gray, 10 μM; black) were applied for each patch after achievement of no inward rectification (white). (B) Comparison of spermine-sensitivity between WT (white bars) and WT/T75M *KCNJ2* (gray bars) at −80 mV (left panel) and 0 mV (right panel). Bars are mean ratios ± SEM of current amplitudes at 0.01 μM and 10 μM spermine, respectively, being normalized to amplitude without spermine. Normalized values were calculated from data in panel A ($n=5$ for each group). There were no significant differences in blockade of the overall K^+ flux either at 0.01 μM or 10 μM spermine.

In the whole-cell patch-clamp experiments (Figs. 3 and 4), CHO-K1 cells were used for recordings of whole-cell currents because of the low level of endogenous K^+ currents. The bath solution (135 mM NaCl, 5 mM KCl, 2 mM $CaCl_2$, 10 mM glucose, 1 mM $MgCl_2$, and 10 mM HEPES, pH 7.4) and the pipette solution (130 mM K-glutamate, 15 mM KCl, 5 mM NaCl, 1 mM $MgCl_2$, 10 mM HEPES, and 5 mM Mg-ATP, pH 7.3) were prepared as described previously [18]. Calculated E_K are −85.7 mV at 22 °C, and −90.0 mV at 37 °C. The tip resistance of the microelectrode (borosilicate glass) filled with the internal solution was 2–4 MΩ; series resistance was 2.5–8 MΩ. After membrane rupture, membrane currents were elicited by 200-ms pulses to +10 mV, from a holding potential of −60 mV. After amplitudes of the monitored currents stabilized, the *I–V* relationships were measured with a series of 200-ms test pulses at 0.1 Hz ranging from −150 mV to +50 mV in 10-mV increments. Instantaneous peak I_{K1} current amplitudes upon applying the test pulses were analyzed to obtain *I–V* curves.

To record macroscopic currents in inside-out patch-clamp, we used HEK293T cells to achieve sufficient protein expression of *KCNJ2* subcloned into the pCXN2-SK vector which has the CAG promoter [18]; this was necessary because we could not obtain sufficient expression of channels in CHO-K1 cells with the vector used for the whole-cell experiments. The pipette resistance was 2–4 MΩ when the pipette was filled with the extracellular solution (16 mM KCl, 120 mM NMDG-Cl, 102 mM HCl, 3 mM $MgCl_2$, 10 mM HEPES, and 4 mM KOH, pH 7.4). The bath solutions (the intracellular side) containing various concentrations of Mg^{2+} or spermine were prepared. The Mg^{2+}- and spermine-free solution consisted of (in mM): 117 KCl, 2 EDTA, 2.8 KH_2PO_4, 7.2 K_2HPO_4, and 6

KOH (pH 7.2). Calculated E_K is −49.5 mV at 22 °C. To assess Mg^{2+}-sensitivities, the concentration of $MgCl_2$ added to the Mg^{2+}- and spermine-free bath solution was 2.2 mM to obtain 0.2 mM free Mg^{2+} concentration; 8.0 mM $MgCl_2$ was used to obtain a 6.0 mM free Mg^{2+} concentration. Spermine-Cl_3 (Nacalai, Japan) was added to the Mg^{2+}- and spermine-free bath solution (final concentrations, 0.01 μM or 10 μM) just before experiments. After obtaining an excised patch, the Mg^{2+}- and spermine-free bath solution was initially applied using a perfusion valve controller (VC-6M, Warner Ins.) to wash out endogenous Mg^{2+} or spermine; currents were continuously monitored by applying 200-ms ramp pulses (1 Hz) from −100 mV to +50 mV (holding potential; −50 mV). After achieving complete disappearance of rectification, various concentrations of either Mg^{2+} or spermine were applied. When current amplitude was stabilized at each concentration of Mg^{2+} or spermine, *I–V* relationships were assessed by applying a series of 200-ms test pulses from −120 mV to +40 mV (10-mV increments, 0.1 Hz). Values of the amplitudes were measured 200 ms after the onset of each test pulse. Data that show apparent run-down were discarded. All data were obtained within 30 min after establishment of the inside-out patch configuration.

2.7. Statistical analysis

Data are shown as mean ± S.E.M. Statistical analysis used the unpaired Student's *t*-test for single comparison, and ANOVA and Bonferroni's test as post-test for multiple comparisons with $P<0.05$ considered significant.

3. Results

3.1. Identification of KCNJ2 mutation

Sequence analysis of the proband's genomic DNA revealed one base substitution, C→T at nucleotide 224 in the *KCNJ2* exon 2. This is expected to cause a non-conservative mutation from Thr to Met at residue 75 (T75M) in the amino-terminus of the Kir2.1 channel (Fig. 1C). Because ATS is an autosomal dominant disorder, affected individuals possess one normal and one mutant *KCNJ2* allele (Fig. 1C). This T75M mutation is inherited in the daughter of the proband who exhibits frequent multifocal premature ventricular contractions. The T75M substitution was not found in 160 informed consents-obtained healthy controls (employees or students at Okayama University).

3.2. Membrane localization of KCNJ2 protein

To investigate the effects of the T75M mutation on membrane localization, GFP-fusion proteins of WT KCNJ2 (WT-GFP) or T75M KCNJ2 (T75M-GFP) were transiently transfected in HEK293T cells (Fig. 2). WT-GFP mainly localized to the plasma membrane, while T75M-GFP failed to localize at the plasma membrane, indicating impaired trafficking by the mutation. When T75M-GFP was co-transfected along with GFP-unfused KCNJ2 (WT), T75M-GFP partially localized to the plasma membrane (Fig. 2A lower panel). The summary of data shows that membrane-localization of T75M-GFP channels plus WT KCNJ2 is as almost same as that of WT-GFP channels (Fig. 2B). These results suggest that WT KCNJ2 restored impaired trafficking of T75M KCNJ2 by forming heteromultimeric channels consisting of WT and T75M KCNJ2.

3.3. Functional characterization of T75M KCNJ2 mutation

We next investigated electrophysiological features of the T75M mutation in CHO-K1 heterologous expression system, because CHO-K1 cells have minimal endogenous outward K^+ currents [16]. Representative instantaneous *I–V* relationships of whole-cell currents recorded from CHO-K1 cells transfected with WT KCNJ2 (Fig. 3A left) show robust expression of the currents with strong inward rectification. In contrast to the WT currents, cells transfected with the T75M KCNJ2 plasmid alone did not yield measurable K^+ currents indicating that the T75M mutation is a loss-of-function one (Fig. 3A center). This result is consistent with impaired localization of KCNJ2(T75M) to the plasma membrane (Fig. 2B). Because ATS patients possess one normal and one mutant *KCNJ2* allele [3–11], we next assessed properties of expressed currents when equal amounts of WT KCNJ2 and T75M KCNJ2 plasmids were co-transfected. When T75M KCNJ2 cDNA was co-transfected with WT KCNJ2 cDNA (WT/T75M), inwardly rectifying K^+ currents were recorded (Fig. 3A, right). The WT/T75M current densities at most of voltages were lower than those induced by transfection with WT KCNJ2 cDNA alone (Fig. 3B, left), indicating that the T75M mutation suppresses expressed inward rectifying K^+ currents in a dominant-negative fashion. In insets of Fig. 3B, enlarged WT and WT/T75M currents between −70 and +30 mV show marked reduction of outward components by the T75M mutation, which is more evident at 37 °C.

To compare the magnitude of the inward rectification between WT and WT/T75M channels, we re-plotted their *I–V* relationships both at 22 °C and 37 °C by normalizing current amplitude at −150 mV, the most negative potential of the test pulses (Fig. 4). Enlarged plots (Fig. 4 inset) clearly show that normalized outward K^+ flux through WT/T75M channels were significantly smaller than those through WT channels between −70 mV and +20 mV, indicating greater inward-rectification of the WT/T75M channels, compared to the WT channels. This analysis led us to hypothesize that the T75M mutation modifies inward rectification of the heteromultimeric channel.

Because inward rectification of the Kir2.1 channels is caused by voltage-dependent block by intracellular Mg^{2+} and polyamines (mostly spermine) [19,20], we next compared Mg^{2+}- and spermine-sensitivity of WT channels and WT/T75M channels. In order to exchange the intracellular solutions quickly, inside-out patch-clamp experiments were carried out in excised patches from HEK293T cells transfected with cDNAs of WT alone or WT/T75M channels inserted into pCXN2-SK vector, giving sufficient expression of the channels in the patches [18]. In contrast with the external K^+ concentration for whole-cell patch-clamp experiments (5 mM), we used a higher external K^+ concentration

(20 mM), which elicits a more positive reversal potential. This condition enabled us to produce comparable driving forces of K^+ efflux as those recorded in the whole-cell experiments with smaller hyperpolarization, and thus to consistently obtain stable recordings from the excised patches [18].

Fig. 5A shows effects of intracellular Mg^{2+} on I–V relationships of the macroscopic currents recorded from cells transfected with WT cDNA alone and those co-transfected with WT and the T75M cDNA. After formation of excised patches, the Mg^{2+}- and polyamine-free bath solution was thoroughly perfused to wash out intrinsic inward rectifying factors. After obtaining the Mg^{2+}-free records, the bath solutions with 0.2 mM $[Mg^{2+}]_i$ as a physiological concentration and 6.0 mM $[Mg^{2+}]_i$ as a high concentration were consecutively perfused, and an I–V relationship at each Mg^{2+} concentration was obtained. When I–V relationships were plotted relative to the amplitude at −120 mV in the absence of $[Mg^{2+}]_i$ (Fig. 5A), in both WT alone and WT/T75M channels, 0.2 mM $[Mg^{2+}]_i$ showed intermediate block of outward currents without affecting inward currents, while 6 mM $[Mg^{2+}]_i$ inhibited both outward and inward components of I_{K1}, showing that $[Mg^{2+}]_i$ at a physiological concentration (0.2 mM) selectively inhibits outward currents [19]. In order to compare the Mg^{2+}-sensitivities at a physiological $[Mg^{2+}]_i$ between WT alone and WT/T75M, expressed current amplitudes at 0.2 mM $[Mg^{2+}]_i$ were normalized to current amplitude without intracellular Mg^{2+} at −80 mV (−30 mV relative to the E_K) for inward currents and at 0 mV (+50 mV relative to the E_K) for outward currents (Fig. 5B). While there was almost no block of inward component at 0.2 mM $[Mg^{2+}]_i$ for both channels, inhibition of outward component at 0.2 mM $[Mg^{2+}]_i$ was significantly greater for the WT/T75M channel than for the WT channel. This result indicates that the T75M mutation increases Mg^{2+}-sensitivity of the channel when it conducts outward K^+ efflux. A high concentration of Mg^{2+} ($[Mg^{2+}]_i$=6 mM) inhibited both inward and outward components for WT/T75M to a greater degree compared to WT alone (Fig. 5B).

We next tested whether sensitivity to spermine is altered by the T75M mutation (Fig. 6). Suppression of outward currents by spermine was investigated in the same manner used to monitor Mg^{2+}-sensitivity. Concentrations of intracellular spermine were 0.01 μM (a low concentration to assess intermediate blockade), and 10 μM (a physiological concentration). Inward currents for both WT alone and WT/T75M channels were not blocked either by 0.01 μM or by 10 μM spermine. Physiological concentration of spermine (10 μM) suppressed outward currents almost completely in both channels. Although spermine at 0.01 μM inhibited outward currents for both WT and WT/T75M, there was no significant difference in the magnitude of current inhibition between the WT alone and WT/T75M channels. Thus, T75M did not modify spermine-sensitivity of the Kir2.1 channel.

4. Discussion

This study identified an amino-terminal *KCNJ2* mutation, T75M, in a Japanese family case of ATS with prolonged QTc intervals and ventricular arrhythmias. In the cellular model, we report three findings regarding biophysical characteristics of T75M; (1) the T75M mutant Kir2.1 impairs trafficking of the channel protein resulting in loss-of-function of the channel; (2) co-expression of the mutant with the WT channel causes dominant-negative effects, while it rescues, at least in part, membrane trafficking of the T75M Kir2.1. We suggest that co-expression of WT and the T75M Kir2.1 channels creates functional heteromultimeric (WT/T75M) channels on the plasma membrane; and most importantly (3) the WT/T75M channels exhibit increased intracellular Mg^{2+}-sensitivity resulting in enhanced inward rectification, which we believe to be the first report of an ATS mutation affecting Mg^{2+}-sensitivity.

ATS mutations are reported to cause loss-of-function by several previous studies: the underlying mechanisms reported so far include trafficking defect [8,10], impaired tetramer assembly [11], and impaired PIP_2 binding [6]. Each of these mechanisms changes the number of available channels on the plasma membrane without affecting gating kinetics. In the present study, we found that the T75M mutation exhibits loss-of-function caused by trafficking defect that is similar to some other mutations [8,10]. Recently, Eckhardt et al. [21] reported in Cos-1 cells that the T75M mutation did not apparently exhibit trafficking defect by a confocal fluorescent microscopic analysis. Because quantitative analysis for the surface expression of the T75M Kir2.1 channel was not provided in their paper, one could not assess whether the magnitude of trafficking defect in Cos-1 cells [21] is different from that in HEK293T cells observed in our experiments.

Electrophysiogical features of the T75M mutation have been characterized in a *Xenopus* oocyte heterologous expression system and in a mammalian cell line, Cos-1. In *Xenopus* oocytes, Davies et al. [22] showed that injection of equal amount of WT and the T75M mutant mRNA induced almost complete suppression of I_{K1}. In Cos-1 cells [21] and in CHO-K1 cells in this study, co-expression of the T75M and the WT KCNJ2 caused a strong, but partial dominant-negative suppression of inward I_{K1}. Thus, in both mammalian cell lines, a strong, but partial dominant-negative suppression of inward I_{K1} is consistently observed in contrast to the finding in *Xenopus* oocytes. For various ion channels, different characteristics have been observed in *Xenopus* oocytes and in mammalian cell lines. One of such examples is that stage V and VI oocytes contain higher concentration of spermine (100–300 μM) compared to mammalian cells (~10 μM), resulting in stronger inward rectification of the Kir2.1 channels [23]. Another example is that aquaporin-2 containing R187C mutation is expressed on the plasma membrane in CHO cells, but not in *Xenopus* oocytes [24]. Expression of the β-subunit of the delayed rectifier K^+ channel KCNE1 alone robust expresses currents in *Xenopus* oocytes, but not in Cos-1 cells, because of the presence of the endogenous α-subunit KCNQ1 in *Xenopus* oocytes [25,26]. However, it is currently unknown whether any of these factors (spermine concentration, differential trafficking, or endogenous proteins) contribute to the differential expression of the WT/T75M hetero-multimeric channels between in *Xenopus* oocytes and in mammalian cell lines, and further examination is certainly required.

Both in Cos-1 cells and CHO-K1 cells, outward direction of I_{K1} currents were strongly suppressed compared to inward I_{K1} currents. We further extended the finding and clarified that the increased inward rectification could be explained by increased sensitivity to intracellular Mg^{2+} in WT/T75M hetero-multimeric channels. In guinea pig ventricular myocytes, Martin et al. [27] found a temperature dependent effect of intracellular Mg^{2+} on I_{K1}. It is of worth noting that we found even greater difference in Mg^{2+}-sensitivity between WT channels and WT/T75M heteromultimeric channels at 37 °C, suggesting that the effects of T75M mutation on gating kinetics of I_{K1} have more significant impact in the physiological condition.

Our electrophysiological data lead us to suggest that inward rectification of WT/T75M heteromultimeric channels is accentuated by increasing intracellular Mg^{2+}-sensitivity without changing sensitivity to spermines at physiological concentrations. One may question the influence of voltage-dependent Mg^{2+}-block on the outward current component in the Kir2.1 channels, because no outward currents were recorded in the intracellular solution containing spermines at a physiological concentration (10 μM) and no Mg^{2+} in both WT and WT/T75M channels (right panel in Fig. 6B). However, it has previously been demonstrated that the voltage-dependent block by intracellular Mg^{2+} has a crucial impact on outward component of the Kir2.1 channels, explained by differential voltage-dependent K_{on} and K_{off} between Mg^{2+}-block and spermine-block [20,28]. In the experimental conditions with both Mg^{2+} and spermines in the intracellular solution, Mg^{2+}-block dominates at relatively weak depolarizing membrane potentials (0 mV to +80 mV relative to the E_K), while spermine-block dominates at more depolarized membrane potentials (>+80 mV relative to the E_K,), resulting in a voltage-dependent switch between Mg^{2+}-block and spermine-block. Partial "shallow" blockade of ion permeation by Mg^{2+} is reflected by an outward hump of the I–V curve in the presence of either intracellular Mg^{2+} or spermines [28]. Thus, even though there was no outward currents in the inside-out patch-experiments with the intracellular solution containing spermines at a physiological concentration (10 μM) and no Mg^{2+}, differential sensitivity to Mg^{2+}-block could contribute to a differential magnitude of outward currents in the whole-cell patch-clamp experiments with intracellular milieu containing both Mg^{2+} and spermines, a more physiological condition than the inside-out patch experiments. However, because the Mg^{2+} consensus binding site (^{172}Asp) locates in the membrane-spanning pore, not in the cytosolic region, it remains unknown how the T75M mutation alters the Mg^{2+} sensitivity. The T75M is predicted to locate between the membrane pore and the cytoplasmic pore [29,30]. The high incidence of ATS mutations (D71V, D71N, T74A, T75A, T75R) in this region [3,6,8,9,21] emphasizes the importance of this region for the channel activity. However, the exact role of the amino-terminus of the Kir2.1 channel is certainly unclear, and requires further examination.

As a prominent cardiac phenotype, the proband manifests bi-directional ventricular tachycardia, unique U-wave, and prolonged QT_c interval (0.5 s) (Fig. 1B). ATS is initially considered as a variant 7 of the inherited familial long QT syndrome (LQT7) [3], but a recent study points out some uncertainty in the designation as LQT7, the apparent prolonged QT_c intervals in ATS is attributable to the U wave in most cases and association of QT_c prolongation in ATS patients is not common (QT_c>460 ms; <20%) [31]. Since the boundary between the T-wave and the U-wave is quite clear in leads II, V4, and V5 of the proband's ECG (see Fig. 1A), the QT_c prolongation in our case appears not to be influenced by the U-wave contamination. In transgenic mouse heart with Kir2.1 containing a mutated signature sequence (AAA for GYG substitution), I_{K1} was reduced by 95%, leading to a significant prolongation of APD [32]. Surface ECG recordings from anesthetized transgenic mice revealed significant prolongation of QT intervals [32]. The ATS-causing substitution at ^{75}Thr to Arg (T75R) possesses a strong dominant negative effect when co-expressed with the same amount of WT Kir2.1 in *Xenopus* oocytes [33]. A transgenic mouse expressing the T75R-Kir2.1 in the heart exhibits prolonged QT_c intervals compared with mice expressing the WT Kir2.1 [33]. These findings suggest that dominant-negative suppression of Kir2.1 per se may cause QT_c prolongation. Influence of Kir2.1 expression level alters voltage dependence of other channels, which may also indirectly affect QT intervals [34]. In addition to these mechanisms, our data may suggest that alterations in the outward hump in the Kir2.1 channel I–V curve by ATS mutations may be one of the factors influencing the QT_c interval. A mutation of the *KCNJ2* causes another type of hereditary arrhythmia syndrome, short QT syndrome type 3 (SQT3) [35]. The mutation G514A of *KCNJ2* causes substitution of ^{172}Asp to Asn (D172N) and results in gain-of-function of the mutant Kir2.1 channels. Interestingly, increases in outward currents without changes in inward currents cause short QT_c interval, suggesting the possible role of the outward current component of Kir2.1 channels on the QT_c interval. Furthermore, in extensive mutation analysis by Tristani-Firouzi et al. [36], the magnitude of reduction in outward I_{K1} currents at −50 mV is well correlated with a prolonged QT_c phenotype. However, Eckhardt et al. [21] reported that the QT_c interval is normal (0.42 s) in a 14-year-old patient with the same T75M mutation, and we found that a 15-year-old daughter of the T75M mutation carrier had borderline QT_c interval (0.44 s). Thus, influence of increased inward rectification of Kir2.1 on the QT_c interval is still controversial, and detailed analysis of mutated channel activity is certainly required for various ATS mutations showing different clinical phenotypes. Simulation of the biophysical properties of the T75M-KCNJ2 mutation using mathematical models of human ventricular myocytes also will be helpful.

Acknowledgments

We thank Dr. Y Kubo (National Institute for Physiological Sciences, Japan) for providing us with pCXN2-SK expression vector. We appreciate the efforts of Dr. Y. Fujiwara (University of California San Francisco, USA) for providing experimental advice and suggestions. We also thank Dr. A.L. Bassett (University of Miami School of Medicine) for proofreading the manuscript.

Funding Sources: This work was supported in part by a Grant-in-Aid for Scientific Research on Priority Areas (17081007, TF), a grant from the Ministry of Education, Science, Culture, Sports and Technology of Japan (17790167, 19689006 JK), health sciences research grants (H18-Research on Human Genome-002) from the Ministry of Health, Labor and Welfare, Japan (TF), and research grants from the Mitsui Life Social Welfare Foundation (TF) and the Mochida Memorial Foundation (JK).

References

[1] Andersen ED, Krasilnikoff PA, Overvad H. Intermittent muscular weakness, extrasystoles, and multiple developmental anomalies. A new syndrome? Acta Paediatr Scand 1971;60:559–64.

[2] Tawil R, Ptacek LJ, Pavlakis SG, DeVivo DC, Penn AS, Ozdemir C, et al. Andersen's syndrome: potassium-sensitive periodic paralysis, ventricular ectopy, and dysmorphic features. Ann Neurol 1994;35:326–30.

[3] Plaster NM, Tawil R, Tristani-Firouzi M, Canun S, Bendahhou S, Tsunoda A, et al. Mutations in Kir2.1 cause the developmental and episodic electrical phenotypes of Andersen's syndrome. Cell 2001;105:511–9.

[4] Ai T, Fujiwara Y, Tsuji K, Otani H, Nakano S, Kubo Y, et al. Novel KCNJ2 mutation in familial periodic paralysis with ventricular dysrhythmia. Circulation 2002;105:2592–4.

[5] Hosaka Y, Hanawa H, Washizuka T, Chinushi M, Yamashita F, Yoshida T, et al. Function, subcellular localization and assembly of a novel mutation of KCNJ2 in Andersen's syndrome. J Mol Cell Cardiol 2003; 35:409–15.

[6] Donaldson MR, Jensen JL, Tristani-Firouzi M, Tawil R, Bendahhou S, Suarez WA, et al. PIP2 binding residues of Kir2.1 are common targets of mutations causing Andersen syndrome. Neurology 2003;60:1811–6.

[7] Andelfinger G, Tapper AR, Welch RC, Vanoye CG, George Jr AL, Benson DW. KCNJ2 mutation results in Andersen syndrome with sex-specific cardiac and skeletal muscle phenotypes. Am J Hum Genet 2002;71:663–8.

[8] Bendahhou S, Donaldson MR, Plaster NM, Tristani-Firouzi M, Fu YH, Ptacek LJ. Defective potassium channel Kir2.1 trafficking underlies Andersen–Tawil syndrome. J Biol Chem 2003;278:51779–85.

[9] Fodstad H, Swan H, Auberson M, Gautschi I, Loffing J, Schild L, et al. Loss-of-function mutations of the K^+ channel gene KCNJ2 constitute a rare cause of long QT syndrome. J Mol Cell Cardiol 2004;37:593–602.

[10] Ballester LY, Benson DW, Wong B, Law IH, Mathews KD, Vanoye CG, et al. Trafficking-competent and trafficking-defective KCNJ2 mutations in Andersen syndrome. Human Mutat 2006;27:388.

[11] Lange PS, Er F, Gassanov N, Hoppe UC. Andersen mutations of KCNJ2 suppress the native inward rectifier current I_{K1} in a dominant-negative fashion. Cardiovasc Res 2003;59:321–7.

[12] Kubo Y, Baldwin TJ, Jan YN, Jan LY. Primary structure and functional expression of a mouse inward rectifier potassium channel. Nature 1993; 362:127–33.

[13] Stanfield PR, Nakajima S, Nakajima Y. Constitutively active and G-protein coupled inward rectifier K^+ channels: Kir2.0 and Kir3.0. Rev Physiol Biochem Pharmacol 2002;145:47–179.

[14] Nakamura TY, Artman M, Rudy B, Coetzee WA. Inhibition of rat ventricular IK1 with antisense oligonucleotides targeted to Kir2.1 mRNA. Am J Physiol 1998;274:892–900.

[15] Niwa H, Yamamura K, Miyazaki J. Efficient selection for high-expression transfectants with a novel eukaryotic vector. Gene 1991;108:193–9.

[16] Kurokawa J, Chen L, Kass RS. Requirement of subunit expression for cAMP-mediated regulation of a heart potassium channel. Proc Natl Acad Sci U S A 2003;100:2122–7.

[17] Bai CX, Namekata I, Kurokawa J, Tanaka H, Shigenobu K, Furukawa T. Role of nitric oxide in Ca^{2+} sensitivity of the slowly activating delayed rectifier K^+ current in cardiac myocytes. Circ Res 2005;96:64–72.

[18] Fujiwara Y, Kubo Y. Ser^{165} in the second transmembrane region of the Kir2.1 channel determines its susceptibility to blockade by intracellular Mg^{2+}. J Gen Physiol 2002;102:677–93.

[19] Matsuda H, Saigusa A, Irisawa H. Ohmic conductance through the inwardly rectifying K channel and blocking by internal Mg^{2+}. Nature 1987;325: 156–9.

[20] Ishihara K, Yan DH, Yamamoto S, Ehara T. Inward rectifier K^+ current under physiological cytoplasmic conditions in guinea-pig cardiac ventricular cells. J Physiol 2002;540:831–41.

[21] Eckhardt LL, Farley AL, Rodriguez E, Ruwaldt K, Hammill D, Tester DJ, et al. *KCNJ2* mutations in arrhythmia patients referred for LQT testing: A mutation T305A with novel effect on rectification properties. Heart Rhythm 2007;4:323–9.

[22] Davies NP, Imbrici P, Fialho D, Herd C, Bilsland LG, Weber A, et al. Andersen–Tawil syndrome: new potassium channel mutations and possible phenotypic variation. Neurology 2005;65:1083–9.

[23] Lopatin AN, Makhina EN, Nichols CG. Potassium channel block by cytoplasmic polyamines as the mechanism of intrinsic rectification. Nature 1994;372:366–9.

[24] Tamarappoo BK, Verkman AS. Defective aquaporin-2 trafficking in nephrogenic diabetes insipidus and correction by chemical chaperones. J Clin Invest 1998;101:2257–67.

[25] Barhanin J, Lesage F, Guillemare E, Fink M, Lazdunski M, Romey G. K_VLQT1 and IsK (minK) proteins associate to form the I_{K_s} cardiac potassium current. Nature 1996;384:78–80.

[26] Sanguinetti MC, Curran ME, Zou A, Shen J, Spector PS, Atkinson DL, Keating MT. Coassembly of K_VLQT1 and minK (IsK) proteins to form cardiac I_{K_s} potassium channel. Nature 1996;384:80–3.

[27] Martin RL, Koumi S, TenEick RE. Comparison of the effects of internal $[Mg^{2+}]$ on I_{K1} in cat and guinea-pig cardiac ventricular myocytes. J Mol Cell Cardiol 1995;27:673–91.

[28] Ishihara K, Ehara T. Two modes of polyamine block regulating the cardiac inward rectifier K^+ current IK1 as revealed by a study of the Kir2.1 channel expressed in a human cell line. J Physiol 2004;556:61–78.

[29] Nishida M, MacKinnon R. Structural basis of inward rectification: cytoplasmic pore of the G protein-gated inward rectifier GIRK1 at 1.8 Å resolution. Cell 2002;111:957–65.

[30] Pegan S, Arrabit C, Zhou W, Kwiatkowski W, Collins A, Slesinger PA, et al. Cytoplasmic domain structures of Kir2.1 and Kir3.1 show sites for modulating gating and rectification. Nat Neurosci 2005;8:279–87.

[31] Zhang L, Benson DW, Tristani-Firouzi M, Ptacek LJ, Tawil R, Schwartz PJ, et al. Electrocardiographic features in Andersen–Tawil syndrome patients with KCNJ2 mutations: characteristic T-U-wave patterns predict the KCNJ2 genotype. Circulation 2005;111:2720–6.

[32] McLerie M, Lopatin A. Dominant-negative suppression of I_{K1} in the mouse heart leads to altered cardiac excitability. J Mol Cell Cardiol 2003; 35:367–78.

[33] Lu C-W, Lin J-H, Rajawat YS, Jeng H, Rami TG, Sanchez X. Functional and clinical characterization of a mutation in KCNJ2 associated with Andersen–Tawil syndrome. J Med Genet 2006;43:653–9.

[34] Wellner-Kienitz M-C, Bender K, Rinne A, Pott L. Voltage dependence of ATP-dependent K+ current in rat cardiac myocytes is affected by I_{K1} and $I_{K(Ach)}$. J Physiol 2004;561.2:459–69.

[35] Priori SG, Pandit SV, Rivolta I, Berenfeld O, Ronchetti E, Dhamoon A, et al. A Novel form of short QT syndrome (SQT3) is caused by a mutation in the KCNJ2 gene. Circ Res 2005;96:800–7.

[36] Tristani-Firouzi M, Jensen JL, Donaldson MR, Sansone V, Meola G, Hahn A, et al. Functional and clinical characterization of KCNJ2 mutations associated with LQT7 (Andersen syndrome). J Clin Invest 2002;110:381–8.

Electrophysiologic characteristics of an Andersen syndrome patient with KCNJ2 mutation

Satoshi Nagase, MD, Kengo Fukushima Kusano, MD, Masashi Yoshida, MD, Tohru Ohe, MD

From the Department of Cardiovascular Medicine, Okayama University Graduate School of Medicine, Dentistry, and Pharmaceutical Sciences, Okayama, Japan.

We report the first case of a patient with Andersen syndrome in whom electrophysiologic study was performed. The patient was a 19-year-old woman with familial periodic paralysis, abnormal QT-U complex, and nonsustained ventricular tachycardia. Mutation analysis revealed a missense mutation in KCNJ2, a component of Kir2.1. Monophasic action potential recordings showed a delayed afterdepolarization (DAD)-like hump in the left ventricle. Initiation of epinephrine-induced premature ventricular contractions always coincided with both the exaggerated DAD-like hump and the U wave. These findings suggest that reduced Kir2.1 current contributes to the development of DAD and ventricular arrhythmias in Andersen syndrome.

KEYWORDS: Andersen syndrome; Electrophysiologic study; Delayed afterdepolarization; Premature ventricular contraction; U wave

(Heart Rhythm 2007;4:512–515)

Introduction

Andersen syndrome is a rare inherited disorder characterized by periodic paralysis, skeletal developmental abnormalities, and long QT with ventricular arrhythmia.[1–5] Andersen syndrome has been reported to be caused by mutations in the KCNJ2 gene encoding the cardiac inward rectifier K^+ channel Kir2.1, a component of the inward rectifier current I_{K1}. I_{K1} stabilizes the resting membrane potential and determines the shape of the terminal portion of the cardiac action potential. Reduced I_{K1} has been suggested to alter late cardiac repolarization and result in prolonged QT or QU interval and ventricular arrhythmias in patients with Andersen syndrome. Similarly, congenital forms of long QT syndrome (LQTS) are caused by mutations in myocardial Na^+ and K^+ channel genes.[6–9] Loss of K^+ channel function or gain of Na^+ channel function lengthens action potential duration and explains the QT interval prolongation and development of ventricular arrhythmias in LQTS. Because these findings support the notion that Andersen syndrome is a disorder of myocellular repolarization, it has been classified as LQT7. Tristani-Firouzi et al[10] reported that KCNJ2 mutations resulted in loss of function and dominant-negative suppression of Kir2.1 channel function. They simulated the effect of reduced Kir2.1 using a ventricular myocyte model to determine the mechanism of ventricular arrhythmia. Their simulation study showed a prolonged terminal phase of the cardiac action potential, delayed afterdepolarizations (DADs), and spontaneous arrhythmias. Ai et al[11] reported on the KCNJ2 mutation T192A, which produced familial periodic paralysis with ventricular arrhythmia and reduced the current amplitude with a dominant-negative effect. We report the first case of a patient with Andersen syndrome and the KCNJ2 mutation T192A in whom electrophysiologic study was performed using the contact electrode technique.[12]

Case report

A 19-year-old female patient was referred to our hospital because of frequent premature ventricular contractions (PVCs) and palpitations. Her father and older brother had suffered from periodic paralysis since their early teens. She was born of a normal pregnancy and delivery, and she had been suffering from periodic paralysis since an early age. Her serum potassium level was within normal limits during a paralytic attack. At age 13 years, she was diagnosed as having Andersen syndrome because of familial paralysis and dysmorphic features such as low-set ears, small chin, and tapering fingers. Treatment with oral acetazolamide was started. At age 19 years, she experienced severe attacks of palpitations. ECG recordings demonstrated frequent PVCs and nonsustained ventricular tachycardia (NSVT) with a bidirectional form and ventricular cycle length of 480 ms (Figure 1A). Multiform PVCs >30,000 beats per day were recorded by 24-hour ambulatory ECG (Figure 1B). She did not experience faintness or syncope. The patient provided written informed consent for genetic and clinical evaluation. The protocol for genetic analysis was approved by the

Address reprint requests and correspondence: Satoshi Nagase, MD, Department of Cardiovascular Medicine, Okayama University Graduate School of Medicine, Dentistry, and Pharmaceutical Sciences, 2-5-1 Shikata-cho, Okayama 700-8558, Japan. E-mail address: snagase@cc.okayama-u.ac.jp. (Received August 1, 2006; accepted October 30, 2006.)

1547-5271/$ -see front matter doi:10.1016/j.hrthm.2006.10.030

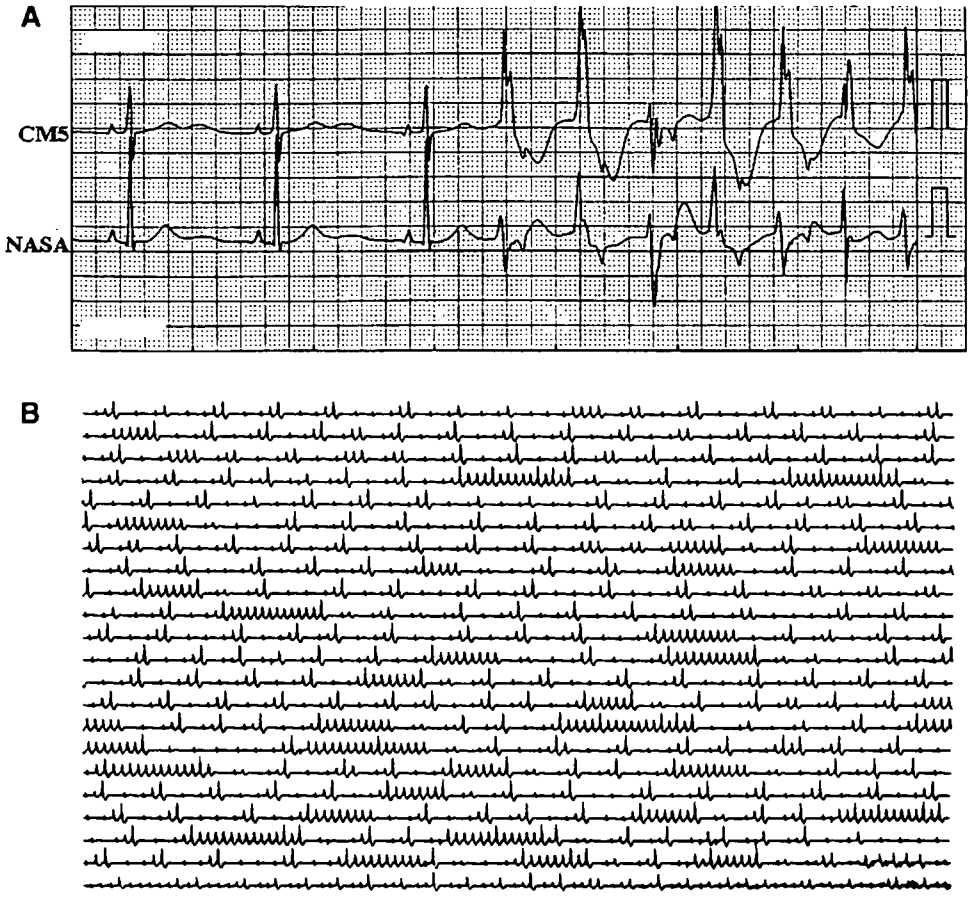

Figure 1 Ambulatory ECG showing frequent premature ventricular contractions (PVCs) and nonsustained ventricular tachycardia (NSVT). **A:** NSVT showed a bidirectional form and ventricular cycle length >480 ms in lead NASA. **B:** Multiform PVCs >30.000 beats per day were recorded by 24-hour ambulatory ECG.

institutional ethics committee and was performed according to institutional guidelines.

Genomic DNA was isolated from leukocyte nuclei by conventional methods. Polymerase chain reaction/single-stranded conformational polymorphism analysis revealed T192A, a heterozygous missense mutation in KCNJ2. Results of routine examinations, including cardiac echocardiography, coronary angiography, right and left ventriculography, and endomyocardial biopsy, showed no evidence of structural heart disease.

Electrophysiologic study

After obtaining informed consent, electrophysiologic study was performed with the patient under local anesthesia and mild sedation. Three 7Fr monophasic action potential (MAP) catheters (MAP–pacing combination catheter, EP Technologies Inc., San Jose, CA) were positioned at the right ventricular apex, right ventricular outflow tract, and left ventricle for MAP recordings. MAPs were recorded simultaneously at the right ventricular apex, right ventricular outflow tract, and left ventricle by the contact electrode technique as described previously.[13–16] MAP signals were amplified and filtered at a frequency of 0.05–500 Hz. Surface ECGs were recorded, and QT interval was measured in all 12 leads. The longest QT interval was used for analysis. After baseline study, epinephrine 10 μg was injected, and MAP and ECG recordings were obtained. Mean QT and QTc intervals of at least four consecutive beats were used for analysis.

Surface ECGs recorded during baseline conditions showed normal QT interval (368 ms) and QTc interval (415 ms; Figure 2A). However, a prominent U wave was observed, especially in leads V_3 and V_4. After epinephrine injection, the U-wave amplitude was exaggerated, and PVCs were induced (Figure 2B). Because the induced PVCs were right bundle branch block type, the PVCs were suspected to originate from the left ventricle. Initiation of PVCs always coincided with the prominent U wave.

MAP recordings showed prolongation of the terminal repolarization phase at the left ventricle and right ventricular apex. The prolonged terminal phase coincided with the U wave on surface ECG (Figures 3A and 4A). After epinephrine injection, MAP recordings showed a prominent afterdepolarization-like hump following the terminal phase of repolarization in the left ventricle (Figure 3B). The afterdepolarization-like hump at the left ventricle always coincided with the U wave, and initiation of induced PVCs always coincided with both the afterdepolarization-like hump and the U wave (Figure 4B).

Discussion

KCNJ2 encodes the inward rectifier K^+ channel Kir2.1, a component of the inward rectifier current I_{K1}. I_{K1} provides a substantial repolarizing current during the terminal repolarization phase of the cardiac action potential and is the

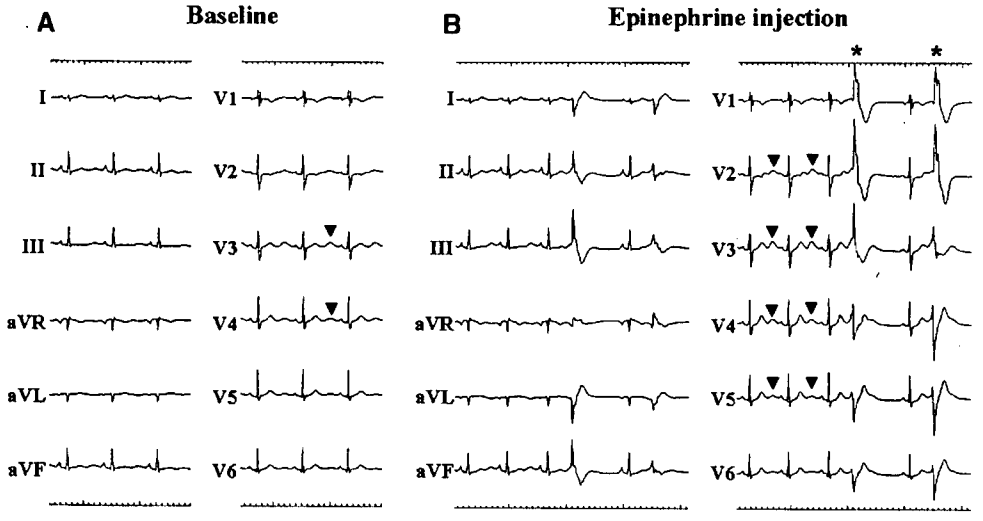

Figure 2 Surface ECGs during baseline conditions (**A**) and after epinephrine injection (**B**). **A:** QT (368 ms) and QTc (415 ms) intervals were within the normal range. However, a prominent U wave (▼) was observed in leads V_2-V_4. **B:** After epinephrine injection, the U wave amplitude was exaggerated and was recorded in leads V_2-V_5. Subsequently, premature ventricular contractions (*) with right bundle branch block type were induced. Initiation of the premature ventricular contractions always coincided with the prominent U wave.

primary conductance controlling the diastolic membrane potential. Mutations affecting I_{Ks}, I_{Kr}, and I_{Na} are the most common causes of LQTS and prolong the plateau phase of the cardiac action potential.[6–9] Prolongation of the plateau phase allows for delayed recovery from inactivation and reactivation of L-type Ca^{2+} channels, which trigger early afterdepolarizations arising from the plateau or early repolarization phases in LQTS.[17–19] However, simulation study of cardiac action potential revealed that reduction in Kir2.1 causes DADs and spontaneous arrhythmias in Andersen syndrome.[10]

This is the first report of electrophysiologic study with MAP recordings in a patient with Andersen syndrome. Clinical studies using MAP recording have suggested that early afterdepolarizations play an important role in the genesis of QT prolongation and ventricular arrhythmias in LQTS. Catecholamine and sympathetic stimulation exaggerate early afterdepolarizations and QT prolongation and subsequently cause ventricular arrhythmias in LQTS.[12–16] In this study, we observed DAD-like humps in a patient with Andersen syndrome and the KCNJ2 mutation T192A. We found that the DAD-like hump always coincided with the prominent U wave on surface ECG. Epinephrine injection exaggerated both the hump and the U wave. Spontaneous PVCs were observed after epinephrine injection, and initiation of PVCs always coincided with both the exaggerated DAD-like hump and the prominent U wave. We spec-

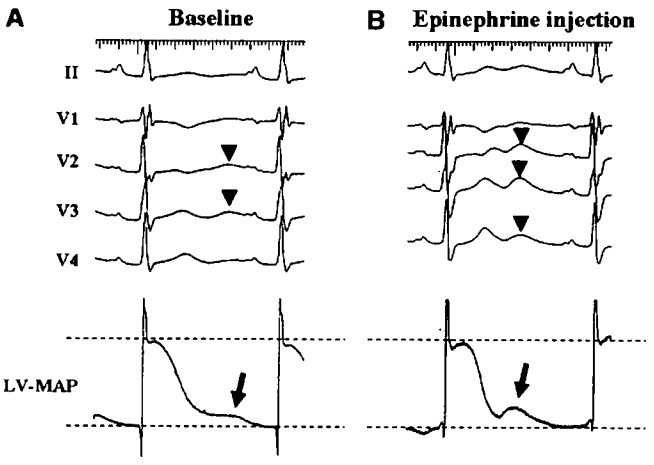

Figure 3 Recordings from surface ECG leads II, V_1 through V_4, and monophasic action potential recordings from the left ventricle (LV-MAP) during baseline conditions (**A**) and after epinephrine injection (**B**). **A:** MAP recording showed prolongation of the terminal repolarization phase at the left ventricle *(arrow)*, and the prolonged terminal phase coincided with the U wave (▼) on surface ECG. **B:** After epinephrine injection, MAP recording showed an afterdepolarization-like hump following the terminal phase of repolarization at the left ventricle *(arrow)*. This afterdepolarization-like hump at the left ventricle coincided with the exaggerated U wave (▼) on surface ECG.

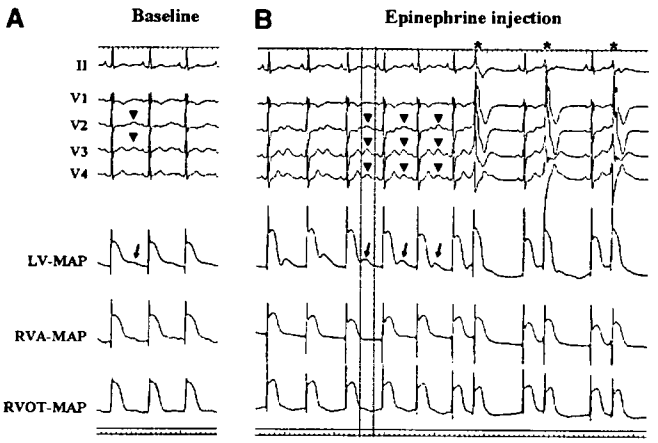

Figure 4 Recordings from surface ECG leads II, V_1 through V_4, and monophasic action potential recordings from the left ventricle (LV-MAP), right ventricular apex (RVA-MAP), and right ventricular outflow tract (RVOT-MAP) during baseline conditions (**A**) and after epinephrine injection (**B**). **A:** MAP recording at the left ventricle *(arrow)* and right ventricular apex showed prolongation of the terminal repolarization phase, which was not apparent at the right ventricular outflow tract. **B:** After epinephrine injection, the U wave (▼) amplitude was exaggerated, and premature ventricular contractions (*) were induced. Initiation of premature ventricular contractions always coincided with the prominent U wave. MAP recordings revealed an afterdepolarization-like hump at the left ventricle *(arrow)*, and the afterdepolarization-like hump coincided with the U wave and with initiation of the induced premature ventricular contractions.

ulate that the U wave recorded on surface ECG represents afterdepolarization in the ventricular endocardial myocardium and that reduced Kir2.1 function in Andersen syndrome results in triggered activity and subsequently ventricular arrhythmia.

The possibility that the DAD-like humps were recording artifacts cannot be completely excluded. However, we do not believe that they were artifacts for the following reasons: (1) MAP recordings maintained a stable configuration, especially at the left ventricle; (2) changes in the DAD-like humps at the left ventricle were closely related to changes in the U waves on surface ECG; and (3) induced PVCs of right bundle branch block type were suspected to originate from the left ventricle, and the prominent afterdepolarization-like humps were recorded from the left ventricle.

In our patient, polymerase chain reaction/single-stranded conformational polymorphism analysis revealed T192A, a heterozygous missense mutation in KCNJ2. Ai et al[11] previously reported the same mutation in another Japanese family manifesting as periodic paralysis and QT prolongation with ventricular arrhythmia, regarded as Andersen syndrome. They also demonstrated using a *Xenopus* oocyte expression system that the T192A mutation reduced the current amplitude of the inward rectifier K^+ channel Kir2.1, with a weak dominant-negative effect. In our patient, reduction of the current amplitude in Kir2.1 might have caused the prominent U wave, afterdepolarization, and subsequently ventricular arrhythmia.

Conclusion

In this case of Andersen syndrome with the KCNJ2 mutation T192A, reduction of the Kir2.1 current contributed to formation of afterdepolarizations and subsequently to development of ventricular arrhythmia. The U wave recorded on surface ECG might represent afterdepolarization in the ventricular endocardial myocardium.

References

1. Andersen ED, Krasilnikoff PA, Overad H. Intermittent muscular weakness, extrasystoles and multiple developmental abnormalities: a new syndrome? Acta Paediatr Scand 1971;60:559–564.
2. Tawil R, Ptacek LJ, Pavlakis SG, DeVivo DC, Penn AS, Ozdemir C, Griggs RC. Andersen's syndrome: potassium-sensitive periodic paralysis, ventricular ectopy, and dysmorphic features. Ann Neurol 1994;35:326–330.
3. Plaster NM, Tawil R, Tristani-Firouzi M, Canun S, Bendahhou S, Tsunoda A, Donaldson MR, Iannaccone ST, Brunt E, Barohn R, Clark J, Deymeer F, George AL Jr, Fish FA, Hahn A, Nitu A, Ozdemir C, Serdaroglu P, Subramony SH, Wolfe G, Fu YH, Ptacek LJ. Mutations in Kir2.1 cause the developmental and episodic electrical phenotypes of Andersen's syndrome. Cell 2001;105:511–519.
4. Zhang L, Benson DW, Tristani-Firouzi M, Ptacek LJ, Tawil R, Schwartz PJ, George AL, Horie M, Andelfinger G, Snow GL, Fu YH, Ackerman MJ, Vincent GM. Electrocardiographic features in Andersen-Tawil syndrome patients with KCNJ2 mutations: characteristic T-U-wave patterns predict the KCNJ2 genotype. Circulation 2005;111:2720–2726.
5. Chun TU, Epstein MR, Dick M 2nd, Andelfinger G, Ballester L, Vanoye CG, George AL Jr, Benson DW. Polymorphic ventricular tachycardia and KCNJ2 mutations. Heart Rhythm 2004;2:235–241.
6. Wang Q, Shen J, Splawski I, Atkinson D, Li Z, Robinson JL, Moss AJ, Towbin JA, Keating MT. SCN5A mutations associated with an inherited cardiac arrhythmia, long QT syndrome. Cell 1995;80:805–811.
7. Curran ME, Splawski I, Timothy KW, Vincent GM, Green ED, Keating MT. A molecular basis for cardiac arrhythmia: HERG mutations cause long QT syndrome. Cell 1995;80:795–803.
8. Wang Q, Curran ME, Splawski I, Burn TC, Millholland JM, VanRaay TJ, Shen J, Timothy KW, Vincent GM, de Jager T, Schwartz PJ, Towbin JA, Moss AJ, Atkinson DL, Landes GM, Connors TD, Keating MT. Positional cloning of a novel potassium channel gene: KVLQT1 mutations cause cardiac arrhythmias. Nat Genet 1996;12:17–23.
9. Sanguinetti MC, Jiang C, Curran ME, Keating MT. A mechanistic link between an inherited and an acquired cardiac arrhythmia: HERG encodes the I_{Kr} potassium channel. Cell 1995;81:299–307.
10. Tristani-Firouzi M, Jensen JL, Donaldson MR, Sansone V, Meola G, Hahn A, Bendahhou S, Kwiecinski H, Fidzianska A, Plaster N, Fu YH, Ptacek LJ, Tawil R. Functional and clinical characterization of KCNJ2 mutations associated with LQT7 (Andersen syndrome). J Clin Invest 2002;110:381–388.
11. Ai T, Fujiwara Y, Tsuji K, Otani H, Nakano S, Kubo Y, Horie M. Novel KCNJ2 mutation in familial periodic paralysis with ventricular dysrhythmia. Circulation 2002;105:2592–2594.
12. Franz MR. Long-term recording of monophasic action potentials from human endocardium. Am J Cardiol 1983;51:1629–1634.
13. Shimizu W, Ohe T, Kurita T, Takaki H, Aihara N, Kamakura S, Matsuhisa M, Shimomura K. Early afterdepolarizations induced by isoproterenol in patients with congenital long QT syndrome. Circulation 1991;84:1915–1923.
14. Shimizu W, Ohe T, Kurita T, Tokuda T, Shimomura K. Epinephrine-induced ventricular premature complexes due to early afterdepolarizations and effects of verapamil and propranolol in a patient with congenital long QT syndrome. J Cardiovasc Electrophysiol 1994;5:438–444.
15. Shimizu W, Ohe T, Kurita T, Kawade M, Arakaki Y, Aihara N, Kamakura S, Kamiya T, Shimomura K. Effects of verapamil and propranolol on early afterdepolarizations and ventricular arrhythmias induced by epinephrine in congenital long QT syndrome. J Am Coll Cardiol 1995;26:1299–1309.
16. Kurita T, Ohe T, Shimizu W, Suyama K, Aihara N, Takaki H, Kamakura S, Shimomura K. Early afterdepolarizationlike activity in patients with class IA induced long QT syndrome and torsades de pointes. Pacing Clin Electrophysiol 1997;20:695–705.
17. Ben-David J, Zipes DP. Alpha-adrenoceptor stimulation and blockade modulates cesium-induced early afterdepolarizations and ventricular tachyarrhythmias in dogs. Circulation 1990;82:225–233.
18. Yan GX, Antzelevitch C. Cellular basis for the normal T wave and the electrocardiographic manifestations of the long-QT syndrome. Circulation 1998;98:1928–1936.
19. Yan GX, Wu Y, Liu T, Wang J, Marinchak RA, Kowey PR. Phase 2 early afterdepolarization as a trigger of polymorphic ventricular tachycardia in acquired long-QT syndrome: direct evidence from intracellular recordings in the intact left ventricular wall. Circulation 2001;103:2851–2856.

tapraid4/zja-jacc/zja-jacc/zja01208/zja4766d08z | moyerr | S=1 | 2/5/08 | Art: 13581

Journal of the American College of Cardiology
© 2008 by the American College of Cardiology Foundation
Published by Elsevier Inc.

Vol. xx, No. x, 2008
ISSN 0735-1097/08/$34.00
doi:10.1016/j.jacc.2007.10.060

Atrial Fibrillation in Patients With Brugada Syndrome

Relationships of Gene Mutation, Electrophysiology, and Clinical Backgrounds

Kengo F. Kusano, MD, Makiko Taniyama, MD, Kazufumi Nakamura, MD, Daiji Miura, PHD, Kimikazu Banba, MD, Satoshi Nagase, MD, Hiroshi Morita, MD, Nobuhiro Nishii, MD, Atsuyuki Watanabe, MD, Takeshi Tada, MD, Masato Murakami, MD, Kohei Miyaji, MD, Shigeki Hiramatsu, MD, Koji Nakagawa, MD, Masamichi Satoshi Sakuragi, MD, Tanaka, MD, Aya Miura, MD, Hideo Kimura, MD, Soichiro Fuke, MD, Wakako Sumita, MD, Satoru Sakuragi, MD, Shigemi Urakawa, MD, Jun Iwasaki, MD, Tohru Ohe, MD, FACC

Okayama, Japan

Objectives The goal of our work was to examine the relationships of atrial fibrillation (AF) with genetic, clinical, and electrophysiological backgrounds in Brugada syndrome (BrS).

Background Atrial fibrillation is often observed in patients with BrS and indicates that electrical abnormality might exist in the atrium as well as in the ventricle. *SCN5A*, a gene encoding the cardiac sodium channel, has been reported to be causally related to BrS. However, little is known about the relationships of atrial arrhythmias with genetic, clinical, and electrophysiological backgrounds of BrS.

Methods Seventy-three BrS patients (49 ± 12 years of age, men/women = 72/1) were studied. The existence of *SCN5A* mutation and clinical variables (syncopal episode, documented ventricular fibrillation [VF], and family history of sudden death) were compared with spontaneous AF episodes. Genetic and clinical variables were also compared with electrophysiologic (EP) parameters: atrial refractory period, interatrial conduction time (CT), repetitive atrial firing, and AF induction by atrial extra-stimulus testing.

Results Spontaneous AF occurred in 10 (13.7%) of the BrS patients and *SCN5A* mutation was detected in 15 patients. Spontaneous AF was associated with higher incidence of syncopal episodes (60.0% vs. 22.2%, $p < 0.03$) and documented VF (40.0% vs. 14.3%, $p < 0.05$). *SCN5A* mutation was associated with prolonged CT ($p < 0.03$) and AF induction ($p < 0.05$) in EP study, but not related to the spontaneous AF episode and other clinical variables. In patients with documented VF, higher incidence of spontaneous AF (30.8% vs. 10.0%, $p < 0.05$), AF induction (53.8% vs. 20.0%, $p < 0.03$), and prolonged CT was observed.

Conclusions Spontaneous AF and VF are closely linked clinically and electrophysiologically in BrS patients. Patients with spontaneous AF have more severe clinical backgrounds in BrS. *SCN5A* mutation is associated with electrical abnormality but not disease severity. (J Am Coll Cardiol 2008;xx:xxx) © 2008 by the American College of Cardiology Foundation

Brugada syndrome (BrS) is a distinct form of idiopathic ventricular fibrillation (VF) characterized by a unique electrographic (ECG) pattern consisting of a right bundle branch block-like morphology and ST-segment elevation in pre-cordial leads (1–3). In addition to the ventricular arrhythmias, atrial arrhythmias are also often observed in this syndrome (4–6), indicating that electrical abnormality might exist in the atrium as well as in the ventricle. We, therefore, speculated that patients with BrS and spontaneous atrial fibrillation (AF) have more advanced disease process.

The human cardiac sodium channel (*SCN5A*) is responsible for the fast depolarization upstroke for the cardiac action potential (7). Mutations in *SCN5A* have been previously discovered in a wide spectrum of cardiac rhythm disorders: the long QT syndrome (8), BrS (7), sick sinus

From the Department of Cardiovascular Medicine, Okayama University Graduate School of Medicine, Dentistry and Pharmaceutical Sciences, Okayama, Japan. This work was supported, in part, by Grant-in-Aid for Scientific Research (No. 18790501), Grant-in-Aid for Young Scientists (No. 17689026) from the Ministry of Education, Culture, Sports, Science and Technology, Japan and Health Sciences Research grants (H18—Research on Human Genome—002) from the Ministry of Health, Labor and Welfare, Japan. This work was also supported, in part, by a grant from the Japan Foundation of Cardiovascular Research, Tokyo, Japan. Drs. Kusano and Taniyama contributed equally to this study.

Manuscript received September 19, 2007; accepted October 19, 2007.

dochead=Clinical Research